

INTERNATIONAL SOCIETY FOR SOIL MECHANICS AND GEOTECHNICAL ENGINEERING



This paper was downloaded from the Online Library of the International Society for Soil Mechanics and Geotechnical Engineering (ISSMGE). The library is available here:

<https://www.issmge.org/publications/online-library>

This is an open-access database that archives thousands of papers published under the Auspices of the ISSMGE and maintained by the Innovation and Development Committee of ISSMGE.

The paper was published in the proceedings of the 13th International Symposium on Landslides and was edited by Miguel Angel Cabrera, Luis Felipe Prada-Sarmiento and Juan Montero. The conference was originally scheduled to be held in Cartagena, Colombia in June 2020, but due to the SARS-CoV-2 pandemic, it was held online from February 22nd to February 26th 2021.

Challenges in analyzing landslide risk dynamics for risk reduction planning

Cees J. Van Westen¹, Felipe Augusto Fonseca Arevalo¹ and Bastian van den Bout¹,

¹ Faculty of Geo-Information Science and Earth Observation (ITC), University of Twente, Enschede, The Netherlands

c.j.vanwesten@utwente.nl

Abstract

This paper discusses approaches to evaluate how landslide risk might change over time. Multi-hazard risk assessment (MHRA) is the quantitative estimation of the spatial distributions of potential losses for an area, of multiple natural hazards with different hazard interactions, with multiple event probabilities, for multiple types of elements-at-risks, and multiple potential loss components. The paper first discusses the various types of hazard interactions in which landslides are involved. An example is presented of a MHRA at district level in Tajikistan for a combination of seven hazard types (earthquakes, floods, windstorms, drought, landslides, mudflows and snow avalanches) and five types of elements-at-risk (Built-up area, buildings, people, agriculture and roads). After discussing problems involved in such types of static MHRA projects, the paper continues with describing the need for analyzing changing multi-hazard risk as a basis for decision-making. These changes may be related to changes in triggering or conditional factors, increasing exposure of elements-at-risk, and their vulnerability and capacity. Dynamic risk can be evaluated on the long term because of changes in climate, land use, population density, economy, or social conditions. Climate change scenarios still contain large uncertainties in the changes in return periods of extreme rainfall events, and their spatial variation in mountainous areas. In addition, feedback mechanisms between climate change and land use change play an important role, but are difficult to incorporate in the risk assessment. Changes in landslide risk might also be occurring in a short time frame, and assessed as a basis for impact based forecasting, and to analyze the consequences of hazard interactions after major events, for instance after the occurrence of wildfires, major earthquakes, volcanic eruptions, or extreme rainfall events, which alter the conditional factors for the occurrence of landslides. An overview is given of the tools available for multi-hazard assessment, stressing the importance for developing integrated physically based multi-hazard models. One of such models, OpenLISEM Hazard, is presented in some more detail. In addition, an overview is given of the tools for multi-hazard risk assessment, stressing the need to incorporate landslide risk within the existing models, as currently this is not taken into account at a sufficient level. One example is given of a Spatial Decision Support System for dynamic multi-hazard analysis, which aims to assist stakeholders in decision making of optimal risk reduction alternatives under various future scenarios. This is further illustrated with a case study for the city of Envigado, near Medellin in Colombia. The OpenLISEM Hazard model is used to generate hazard scenarios for flood, landslides, and debris flows for different return periods of triggering rainfall. Building footprints are updated and classified into occupational types, and structural types, and absolute vulnerability curves were generated. Current multi-hazard risk is analyzed. After that several future scenarios of climate change and population change are outlined, for which the changing risk is analyzed. Finally, three alternatives for risk reduction are presented, their risk reduction is calculated, and eventually the optimally performing alternative under different future scenarios is selected.

1 INTRODUCTION

Large-scale disasters (e.g. earthquakes, cyclones, floods, volcanic eruptions and forest fires) cause widespread losses to society, leading to direct and indirect social and economic losses (EM-DAT, 2020). After years with large losses by earthquakes (e.g. 2008 China, 2010 Haiti, 2015 Nepal), the years 2017, 2018 and 2019 were characterized by tropical storms and wildfires, causing losses of 300, 139 and 150 billion Euro respectively (MunichRe, 2020). These events also have a large impact on the natural environment, and critically change the conditions related to vegetation, hydrology and active geomorphological processes leading to new hazards, or increased intensity and frequency of existing hazards. When such events occur in mountainous regions they will often result in an increased activity of mass movement.

Understanding the role of landslide dynamics in multi-hazard risk is in line with the Priority Areas of the Sendai framework. Priority 1 (Understanding disaster Risk) indicates *“Disaster risk management should be based on an understanding of disaster risk in all its dimensions of vulnerability, capacity, exposure of persons and assets, hazard characteristics and the environment. Such knowledge can be used for risk assessment, prevention, mitigation, preparedness and response”* (UNDRR, 2020). Priority 3 (Investing in disaster risk reduction for resilience) stresses the importance of investing in disaster risk reduction, which should be based on analyzing the current level of risk, and how the risk could be reduced through the implementation of structural and non-structural measures. This requires an evaluation of risk dynamics. Also in Priority 4 (Disaster Preparedness and Build-Back-Better), disaster risk assessment forms a crucial component of the disaster preparedness and reconstruction phases (UNDRR, 2020)..

Landslides often do not feature among the key hazards to address in these programmes. Landslide-related damage, however, is much more prominent than what would appear from the official disaster records. In a global study for the period between 2004 and 2016, Froude and Petley (2018) concluded that 56,000 people were killed during 4,900 landslide events. The reported number by Froude and Petley (2018) is substantially larger than the 12,000 recorded in EM-DAT for the same period (EM-DAT, 2020). This is due to the inclusion thresholds used for recording disaster events, which excludes landslides with less than 10 casualties, and

because it is often grouped under the main disaster event that triggered it (e.g. earthquake, cyclone). The secondary role of landslides is also reflected in the frameworks for multi-hazard risk, and the tools for multi-hazard risk assessment (e.g. HAZUS and CAPRA), which often have at best a sketchy role for landslide hazard and risk assessments.

2 MULTI-HAZARD INTERACTIONS

One of the difficult issues in the inclusion of landslides in multi-hazard frameworks is related to hazard interactions. Multi-hazard events occur when multiple hazardous processes influence the behavior of others in a significant way. Figure 1 gives an overview of hazard relationships, in which hazard types are grouped according to their triggering mechanism, and according to the specific physiographic region in which they occur. There are different ways in which hazards may interact, which will have an important consequence for the risk assessment (Bell & Glade, 2004; Kappes et al., 2012; Gill and Malamud, 2014; 2017; Van Westen & Greiving, 2017) :

- A. **Independent events:** several types of hazardous processes may be completely unrelated to each other with respect to their origin and trigger. The occurrence of one event does not have an influence on the other. The risk due to the two hazardous processes could be added for the same area. For example, landslides and snowstorms affecting the same region, each with its own intensity-frequency relationship. Often processes that seem independent at first sight are not so independent after all. In the previous example, rapid snowmelt after a snowstorm might be trigger landslides.
- B. **Compounding events:** hazardous processes that are unrelated may occur in sequence, close to each other, so that the damage caused by one event is worsened by the subsequent unrelated event. For example: landslides and debris flows that affect the road network in a forested area that is subsequently affected by forest fires, so that rescue and firefighter operations are less effective.

C. **Coupled events:** hazardous events might share the same trigger, may occur simultaneously and could affect the same area. They might also

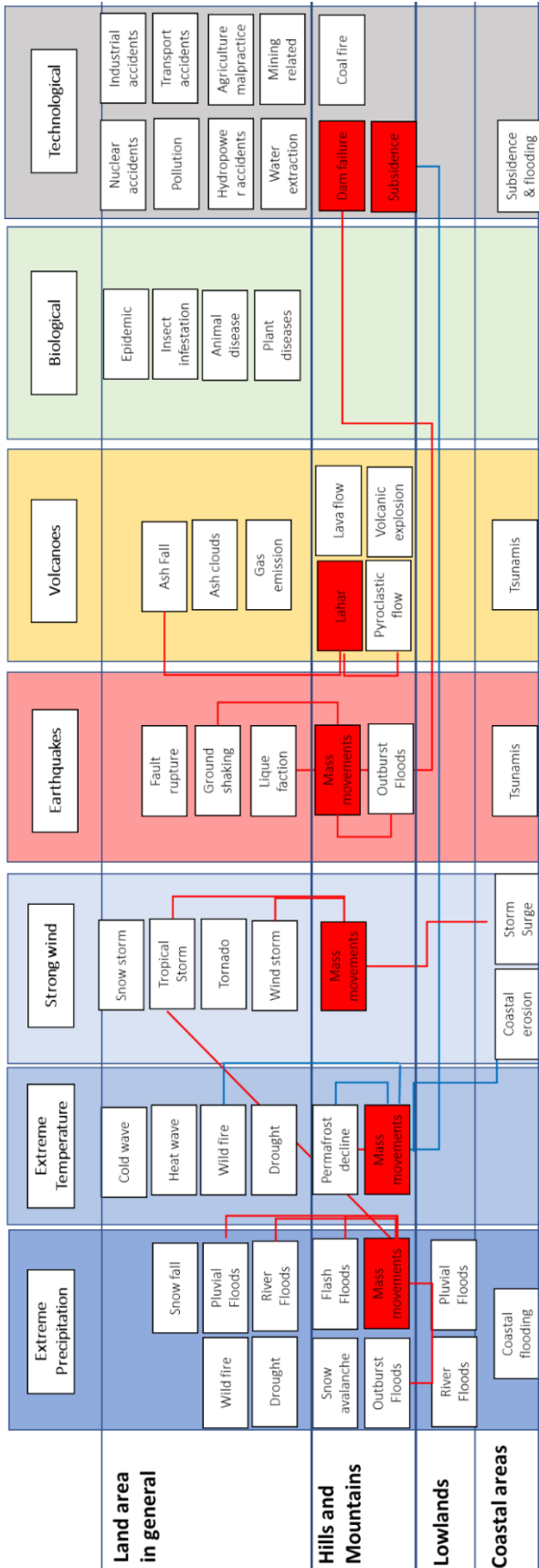


Figure 1. Possible hazard relationships.

influence each other during the process itself. For example, during the same extreme rainfall event in mountainous areas the sediments produced by landslides interact with rainfall runoff processes, and may cause debris flows, hyperconcentrated flood and flashflood periods in the same watershed, affecting the same areas. In this case, the hazard and risk assessment should take into account the combined effect of the hazardous processes.

D. **Cascading events:** these hazardous processes occur in sequence, where one process triggers the second and the second the third. These are therefore also called domino effects. An example of such a cascade is a rockfall or large landslide that catastrophically deposits within a lake, causing a flood wave (Byers et al., 2018). The essence is that one process directly initiates a follow-up process, which would not have occurred if it had not been triggered by the previous event.

E. **Conditional events:** these hazardous events change the conditions of the landscape in such a way that the susceptibility/likelihood and/or intensity of other hazardous processes increases substantially. The conditions may be related to the vegetation characteristics, topography, material characteristics or other factors that play a role in the occurrence of the hazardous processes. An example of conditional events are wildfires, which modify the vegetation and soil characteristics, making the landscape more susceptible to landslides and flashfloods (DeGraff, 2018). The change of conditions can be abrupt (as in the previous example) or gradual over a longer period of time (e.g. as is the case in global warming in arctic or alpine regions, reducing the layer of permafrost, and making the terrain gradually more susceptible to landslides). Some authors use the terms “delayed cascading” events to refer to processes that trigger other ones with a time in between.

One of the most complex hazard interactions involving landslides is related to earthquakes in mountainous environments causing many hazard relationships, including coseismic landslide dams, dam break floods, and post-earthquake landslides and debris flows (Fan et al., 2019; 2020). Another important set of hazard interactions with mass movements are those that are triggered during tropical storms in mountainous environments. The interaction of wind in forests, adding tree debris to the sediments contributing to the stream network resulting from landslides, and the rainfall-runoff processes, generate specifically hazardous

conditions that require integrated modelling approaches.

3 MULTI-HAZARD RISK ASSESSMENT

A generally accepted definition of multi-hazard risk still does not exist (Marzocchi et al., 2009; Komendatova et al., 2014; Gallina et al., 2016). Schmidt et al. (2011) use the following definition: “Quantitative estimation of the spatial distributions of potential losses for an area (a confined spatial domain), multiple (ideally all) natural hazards, multiple (ideally a continuum of) event probabilities (return periods), multiple (ideally all) human assets and multiple potential loss components (for each of the assets, e.g. buildings, streets, people, etc.).”

Risk is the multiplication of probability, exposure and vulnerability. Landslide risk assessment reviews can be found for example in Fell et al. (2008) and Corominas et al. (2014).

For independent hazardous processes, the multi-hazard risk can be approximated by the integral in equation 1.

$$Risk = \sum_{\text{All Hazards}} \left(\int_{P_i=0} P_{(T|HS)} * (\sum_{\text{All EaR}} (P_{(S|HS)} * (A_{(ER|HS)} * V_{(ER|HS)})) \right) \quad (1)$$

In which: $P_{(T|HS)}$ = the temporal probability of a certain hazard scenario (HS). A hazard scenario is a hazard event of a certain type (e.g. debris flow) with a certain magnitude and frequency; $P_{(S|HS)}$ = the

spatial probability that a particular location is affected given a certain hazard scenario; $A_{(ER|HS)}$ = the quantification of the amount of exposed elements-at-risk, given a certain hazard scenario (e.g. number of people, number of buildings, monetary values, hectares of land) and $V_{(ER|HS)}$ = the vulnerability of elements at risk given the hazard intensity under the specific hazard scenario (as a value between 0 and 1).

The equation can be valid for natural hazards that are not related in terms of triggering factors, or causal relationships, but would not allow calculating the risk of compounding, coupled or cascading hazard. For particular situations, complex approaches for multi-hazard risk assessment have been proposed (Newman et al., 2014; Gallina et al., 2016; Terzi et al., 2019). Most of these may be useful in specific cases, but would still be difficult to implement in most regions due to data scarcity.

This is illustrated with a practical example of a multi-hazard risk assessment procedure used for a national scale risk assessment project in Tajikistan (Van Westen et al., 2020). The aim is to generate risk information for the districts in the country, for a combination of seven hazard types (earthquakes (EQ), floods (FL), windstorms (WS), drought (DR), landslides (LS), mudflows (MF) and snow avalanches (SA)) and five types of elements-at-risk (Built-up area, buildings, people, agriculture and roads) (Figure 2 and Figure 3).

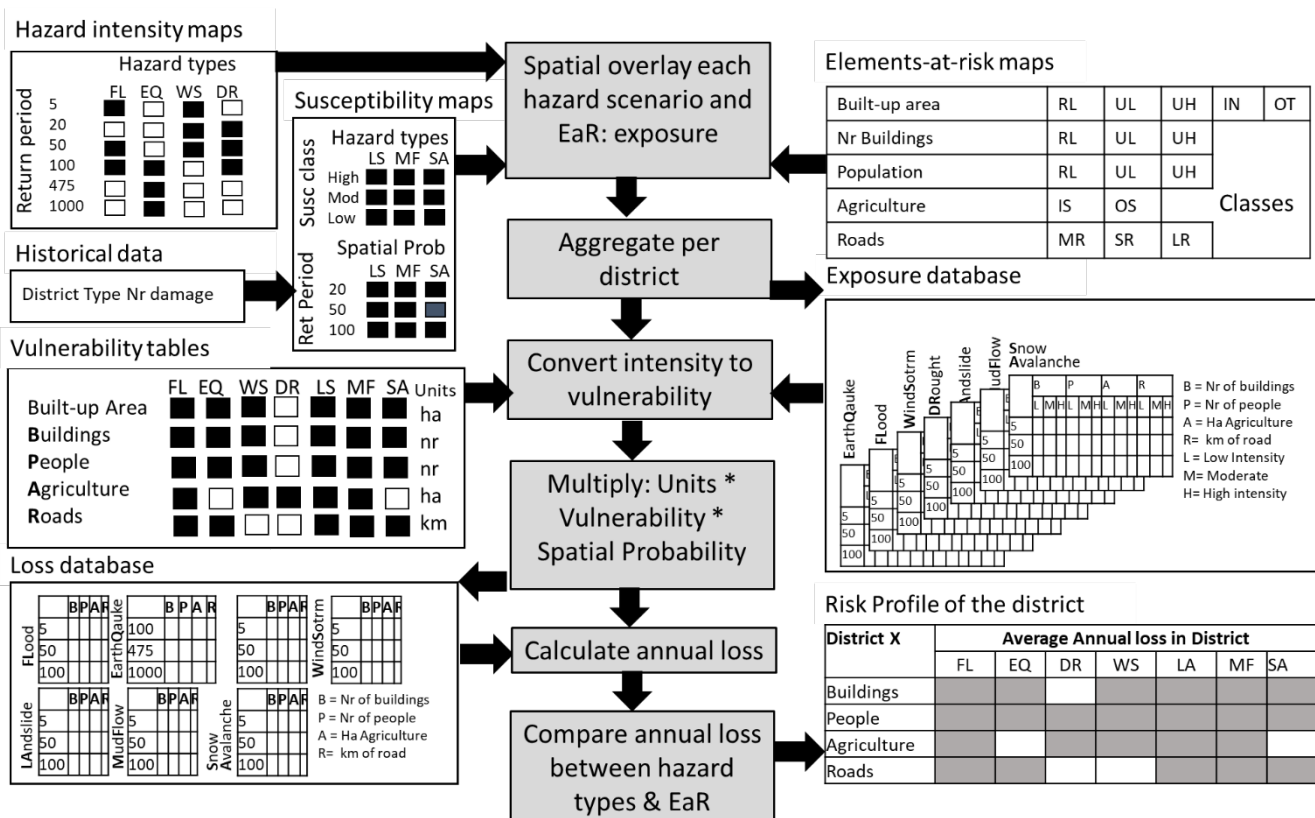


Figure 2: Flowchart for multi-hazard risk assessment for national scale MHRA study in Tajikistan (Van Westen et al.,

The hazard intensity such as water depth (flooding), acceleration (earthquake), speed (wind), and SPI (drought), was modelled using separate modelling approaches. The frequency of these hazards were estimated from historical records of precipitation, wind speed and earthquakes. The return periods for which intensity information was available differed for the various hazard maps (See Figure 2). For instance, earthquake hazard maps were generated for return periods (100, 475 and 1000 years) that are much larger than for other hazards such as flooding. For three hazard types (landslides, mudflows and snow avalanches), it was not possible to create intensity/frequency maps due to lack of data, and appropriate modelling tools given the size of the study area. For these only susceptibility maps were made using a hybrid model (statistical and heuristic) that show zones with a relative likelihood of occurrence of hazardous phenomena, without a clear indication of the frequency and intensity. For these hazard types, the spatial probability that a particular area would be impacted was estimated based on the ratio of the expected area of future events (based on historical records) and the area of the susceptibility classes. Due to the absence of spatially referenced historical inventories, and the overall incompleteness of the historical records, the spatial and temporal probability was very uncertain. All hazard maps were classified into three classes of frequency and three classes of intensity (or susceptibility and spatial probability). This classification was done taking into account the damaging effects of the hazard, where the high-class boundaries were chosen such that they represent different danger levels with respect to buildings and people.

We considered the hazard types, and their expected impacts within the districts, in an independent manner, which means that we were not able to model the hazard interactions that could take place. These might lead to cascading hazards (e.g. earthquake-triggered landslides, floods resulting from landslides damming rivers), or the occurrence of one type of hazard might lead in time to another (e.g. wildfires which lead to mudflows in due course of time). The modelling of these hazard interactions remains a major scientific challenge and cannot be carried out over large areas, such as an entire country.

In this study, elements-at-risk were limited to buildings, population, agricultural areas and roads. Roads were obtained from OpenStreetmap. Agricultural areas were obtained through digital image processing, combined with collaborative

mapping. Built-up areas were obtained using a cloud-based machine-learning algorithm. The built-up areas were subdivided into homogeneous zones with similar building characteristics through extensive collaborative image mapping, and subdivided into five classes (rural buildings (RL), urban low rise building (UL), urban high rise buildings (UH), industrial areas (IN), and others (OT)) (See Figure 2). The building footprints from OpenStreetMap, which were only available for a few areas, were used in combination with an extensive sample of about 500 homogenous built-up areas to estimate the building density within the three residential classes. Census data were used in combination with the modelled number of buildings and building types (including number of floors and total floor space) to estimate the number of people per homogeneous built-up unit.

Exposure was calculated by spatially overlaying the hazard maps with the elements-at-risk maps, and with the administrative boundaries of districts, to obtain the area of built-up zones, the number of buildings and people, the area of agricultural land, and the length of roads within each district exposed to a certain level of hazard intensity (or susceptibility). Not all combinations of hazards and elements-at-risk were considered relevant to evaluate (e.g. the effect of drought on roads, or earthquakes on agriculture land). The exposure analysis resulted in a database with data per district (See Figure 2).

Vulnerability curves from literature (Papathoma-Köhle, 2016; Ciurean et al., 2017; Fuchs et al. 2018; CAPRA, 2020) were consulted and converted into vulnerability matrices, that displayed the damage ratio (percentage of exposed elements-at-risk that would be destroyed) for each hazard type and each intensity class. For those hazard types (landslides, mudflows and snow avalanches) for which no hazard intensity information was available, exposed elements were assigned a vulnerability value of 1. The vulnerability matrices were used in combination with the exposure data to convert the intensity into vulnerability, which was then multiplied by the spatial probability. This resulted in the loss database where losses are stored for each combination of hazard type/frequency class and elements-at-risk type.

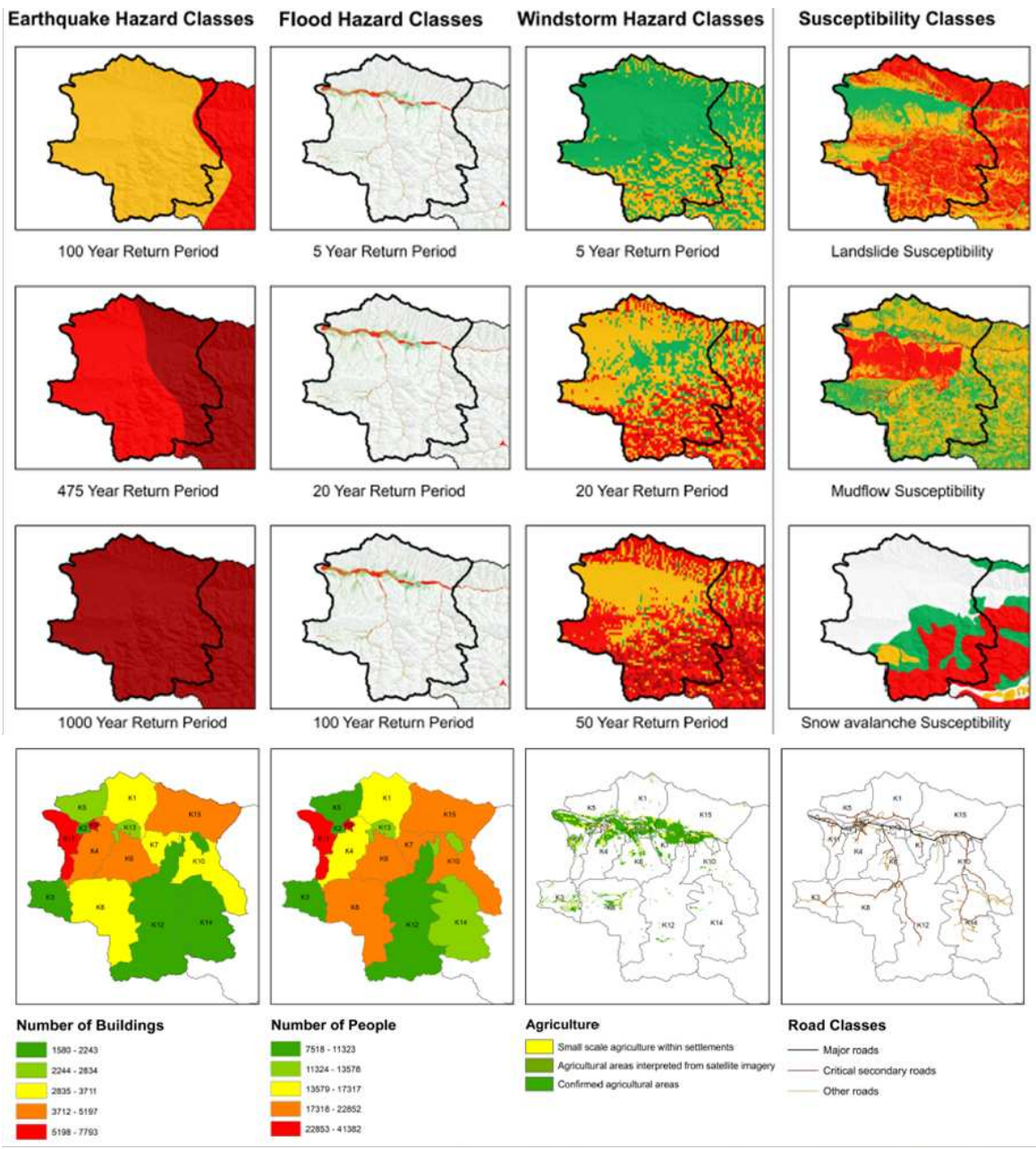
Average annual losses were calculated for each hazard type and element-at-risk combination using the three available frequency and loss values, and applying a simplified method to assess the area under the risk curve.

The risk values are very different for the various hazard & elements-at-risk. For instance expected losses of agriculture to windstorms in hectares, cannot

be added to expected kilometres of road flooded.

Therefore we use them as individual indicators for each district, which can be compared in order to make a prioritization of districts with respect to multi-hazard risk.

Figure 3: Example of risk profile for one of the districts (Panjakent) in Tajikistan with hazard maps, elements-at-risk and screenshot of the risk platform (<http://tajirisk.ait.ac.th/>)



Tajikistan Multihazard Data Portal

Home Hazard Map EAR Data Exposure Map Risk Map Risk Profiles About Us

Please choose administrative unit that you want to generate a report

Region: Select Region
 District: Select District
 Jamoat: Select Jamoat
 Risk: Select Risk Type
 A/P: Select Absolute/Percentage

| # | EarthQuake | Flood | Landslide | Snow | Wind | Drought | All |
|-------------|--------------------------|--------------------------|--------------------------|--------------------------|--------------------------|--------------------------|--------------------------|
| Building | <input type="checkbox"/> | <input type="checkbox"/> | <input type="checkbox"/> | <input type="checkbox"/> | <input type="checkbox"/> | <input type="checkbox"/> | <input type="checkbox"/> |
| Population | <input type="checkbox"/> | <input type="checkbox"/> | <input type="checkbox"/> | <input type="checkbox"/> | <input type="checkbox"/> | <input type="checkbox"/> | <input type="checkbox"/> |
| Roads | <input type="checkbox"/> | <input type="checkbox"/> | <input type="checkbox"/> | <input type="checkbox"/> | <input type="checkbox"/> | <input type="checkbox"/> | <input type="checkbox"/> |
| Agriculture | <input type="checkbox"/> | <input type="checkbox"/> | <input type="checkbox"/> | <input type="checkbox"/> | <input type="checkbox"/> | <input type="checkbox"/> | <input type="checkbox"/> |

Generate report Select all Clear all selection Generate report for selected features

Although the example shown above deals with large areas, it is indicative of the problems involved when analysing the mass movement aspect of multi-hazard risk:

- Incomplete historical inventories to make a clear relation between trigger events and landslide frequency. For instance, only for one earthquake (1949 Khait earthquake) an earthquake-induced landslide inventory was available, and not rainfall-induced inventories;
- Unavailability of factor maps related to geotechnical and hydrological properties to be able to use physically-based hazard models for mass movements;
- Insufficient density of meteorological stations and lengths of measurements to make a proper rainfall frequency analysis;
- Inability to represent the intensities of different landslides as a function of landslide type;
- Insufficient data to characterize individual buildings according to structural types and number of floors;
- Unavailability of appropriate vulnerability curves for landslide phenomena.
- One of the research challenges is to define which risk metrics could and should be used in the decision making process, depending on many factors such as the risk governance framework, risk acceptability criteria, the objective of the risk assessment, the stakeholders, the scale of analysis, the data availability. Many types of risk could be analyzed (e.g. economic, population, direct, indirect, sectoral, public, private etc.)

For smaller areas in data rich environments, these problems might be less severe, but are still significant as will be shown later on in the case study dealing with changing multi-hazard risk in a part of Medellin, Colombia.

4 CHANGING MULTI-HAZARD RISK FOR DECISION MAKING

The quantification of changing multi-hazard risk, not only requires information on current hazards elements-at-risk and vulnerability, but also how these might change in future. This is a multi-disciplinary research, which requires collaboration with social scientists, engineers, and economists. Future changes might be relatively slow, allowing ample time to collect information, or fast, such as after disaster events, where data changes rapidly.

4.1 Analyzing slow changes

Possible future scenarios can be formulated that project possible changes related to climate, land use

change or population change due to global and regional changes, and which are only partially under the control of the local planning organizations. The stakeholders might like to evaluate how these trends have an effect on the hazard interactions, exposed elements-at-risk and their vulnerability and how these would translate into different risk levels.

4.1.1 Climate change scenarios.

In order to evaluate the impact of climate change on multi-hazard risk with landslide interactions, the stakeholders require the involvement of experts that indicate which climate change scenarios would be evaluated. The expected effects in terms of changes in frequency and magnitude of hydro-meteorological triggers should be analyzed, but also possible new hazards that results from climate change (e.g. increased landslide activity in areas with permafrost decline), or other feedback loops (e.g. increased forest fire activity leading to more debris flows, e.g. Bovolo et al., 2009).

The IPCC reports “*that heavy precipitation events have increased in frequency, intensity, and/or amount since 1950 and that further changes in this direction are likely to very likely during the 21st century*” (IPCC 2012). The recent IPCC special report on Climate Change and Land (IPCC, 2019) indicated that climate projections of precipitation are less robust than for temperature as they involve processes of larger complexity and spatial variability. There is evidence that the number of heavy rainfall events is increasing, while the total number of rainfall events tends to decrease. IPCC (2019) also concludes that, although there is general agreement on the expected increase in landslide activity due to the intensification of rainfall, the actual empirical evidence for this is still lacking (Huggel et al., 2012; Gariano and Guzzetti 2016). Froude and Petley (2018) in a study on landslide related victims did not see an overall increasing trend, although the number of persons killed in landslides caused by human activities, such as mining, has increased in the last decade. Coe and Codt (2012) and Gariano and Guzzetti (2016) present reviews on possible approaches for assessing the impact of climate change on landslide hazards (slope stability modeling, statistical modeling, regional modeling, historical analysis of landslide and climate records, and analysis of landslide paleo-evidences). For example, Alvioli et al. (2018) used a combined hydrological and slope stability model (TRIGRS) in combination with downscaled synthetic rainfall fields from regional climate model projections to model changes in rainfall thresholds and area-frequency distributions. The number of

modelling studies that try to quantify the possible change of landslide-related multi-hazard risk is still limited. Terzi et al. (2019) give a review on modelling approaches for climate change adaptation in mountainous regions, and indicate five possible innovative approaches (Bayesian networks, agent-based models, system dynamic models, event and fault trees, and hybrid models), but conclude that there are still few applications.

4.1.2 *Land use change scenarios.*

Next to evaluating the effect of climate change stakeholders also need to consider the possible changes in landslide risk, under certain land use change scenarios. This requires the involvement of experts that would indicate possible land use changes based on macro-economic and political developments, which would be translated into local changes. The future land use scenarios would also involve possible changes in population, which should also be taken into account. Models for land use change are reviewed by Verburg et al. (2019). Malek et al. (2019) made an extensive literature review of case studies on land use change modelling. Various studies have demonstrated the importance of land use change in the frequency and density of landslides (e.g. Glade, 2003; van Beek and Van Asch, 2004; Promper et al., 2014).

4.1.3 *Planning of risk reduction measures*

Risk analysis is also relevant to support stakeholders in the evaluation of the best risk reduction alternative, or combination of alternatives. Structural measures refer to any physical construction to reduce or avoid possible impacts of hazards, which include engineering measures and construction of hazard-resistant and protective structures and infrastructure. The strategy is to modify or reduce the hazard. Non-structural measures refer to policies, awareness, knowledge development, public commitment, and methods and operating practices, including participatory mechanisms and the provision of information, which can reduce risk and related impacts. Risk analysis as the basis for spatial planning is traditionally seen as the key for preventive measures (Greiving et al., 2006). In the physical development plans of national and local levels, also possible future developments will be outlined and priorities for development indicated which have implications for the spatial distribution of land use and population.

After defining possible alternatives, the new risk level is analyzed, and compared with the existing one to estimate the level of risk reduction. Depending on the risk metric a number of methods

can be applied to compare risk reduction alternatives: such as Cost-Benefit analysis (when risk reduction, investment and maintenance costs can be compared (Narasimhan et al., 2016), Cost-Effective Analysis (when risk cannot be quantified in monetary terms due to lack of data), and Spatial Multi-Criteria Evaluation (when both costs and benefits are expressed qualitatively). The research challenge is develop this approach for areas with relative data scarcity, and optimally link hazard models with risk models

In practice combinations of climate change, land use change scenarios and planning alternatives should be developed, and the possible changes should be expressed for certain years in the future, and are considered as a basis for risk reduction planning and climate change adaptation.

4.2 Analyzing rapid changes

Many activities related to the application of MHRA in Disaster Management focus on the prevention phase, where there is enough time to develop the scenarios, collect the data and carry out the analysis. However, also in the preparedness and response phases, rapid decision making is needed that requires information on fast changing multi-hazards.

4.2.1 *Impact-based forecasting*

Impact Based Forecasting (IbF) is a procedure to provide predictions on the possible impact of disasters based on forecasts of measurable precursors in an Early Warning System. This impact is analyzed based on a combination of available existing data (e.g. population distribution, agricultural areas, infrastructure) and continuously changing data (e.g. weather forecasts). It is part of Forecast-Based Financing (FbF), which enables access to humanitarian funding for early action based on in-depth forecast information and risk analysis (FbF, 2020).

Landslide early warning is much more complicated compared to other types of natural hazards, as landslide initiation locations are difficult to predict, both in space and in time (Corominas et al., 2014). Current initiatives on landslide early warning mostly focus on the establishment of a regional threshold for landslide warning, which does not include a spatial prediction of the types, numbers and volumes of landslides, needed as a basis for subsequent risk assessment. For rainfall-induced landslides NASA has been working for some time on the Landslide Hazard Assessment for Situational Awareness (LHASA) method, which incorporates a

global landslide susceptibility map with rainfall estimates from satellite data (TRMM and GPM) and global and regional rainfall thresholds (Kirschbaum and Stanley, 2018). Also the application of satellite-based rainfall products, in combination with rainfall forecasts and physically-based models for soil moisture and slope stability have resulted in a number of operational Landslide EWS (Devoli et al., 2018; Piciullo et al., 2018). However, the parameterization of these methods at a local level remains a major problem, leading to a major overestimation of instability, which renders it less useful in landslide early warning, and impact based forecasting.

Also in the field of earthquake-induced landslides, there have been attempts to generate rapid information on expected landslide distribution, following an earthquake. Early warning for earthquakes is not an operational procedure and therefore impact based forecasting will also not be possible. However, in order to support rescue planning it is important to assess the possible landslide distribution as soon as an earthquake has occurred, before landslides can be mapped using satellite images. Earliest attempts were made by Godt et al. (2008), using a hybrid model that included a basic Newmark model approach. Statistical models have proven to be more adequate as was demonstrated by Nowicki Jesse et al. (2018) and Tanyas et al. (2019). The model of Jesse et al. (2018) is used by the U.S. Geological Survey (USGS) in combination with PAGER population data to give an estimation of the number of people that might be affected by earthquake-induced landslides (USGS, 2020).

4.2.2 Recovery planning

Risk changes very rapidly in the recovery phase, which includes both rehabilitation and reconstruction, as well as full functional recovery. Depending on the scale of the disaster, but also the resilience of the affected society and involved institutions, recovery takes different trajectories. Those can range from a more rapid or a slower recovery to pre-event levels, partial recovery, or a slow abandoning of the disaster area, none of which are desirable outcomes. Recovery might also be affected by multiple/successive event in the affected area and the research should focus primarily on those situations (Zobel and Khansa, 2014). The occurrence of a disaster event changes the conditions and makes the area more susceptible to other hazards or similar hazards may affect the same

area during the recovery phase. The combination of these factors can be analyzed and quantified. Recovery, and in particular reconstruction, should be aligned with the principles of sustainable development and “build back better”, to avoid or reduce future disaster risk. Therefore, it should be carried out on the basis of a more precise assessment of damage and of the changes in hazard and risk. Large-scale disasters have a major effect on the environment, changing the landscape, landforms, active processes, and vegetation in such a manner that new types of hazards may occur in locations where they did not happen before, or the frequency and intensity of existing hazards might increase substantially. Access to accurate and up-to-date information is one of the key challenges in post-disaster reconstruction planning. A wide range of new geospatial data is required to portray the new topography, vegetation, and human environment and to monitor the changes that take place. Assessing 3D changes over a timeline introduces the fourth dimension 4D (time), a crucial factor for decision-making and for monitoring actions focused on restoring and improving the status of the disaster affected area. Pre-event data can be collected from existing sources i.e. topographic maps and Earth Observation (EO) satellite imagery. Post-event data should be surveyed on demand, with ad-hoc campaigns, with airborne, piloted or remotely piloted aircrafts, or terrestrial surveys (Pirotti et al., 2015). Crowdsourcing complements computer-based automatic information extraction from 4D remote sensing data, though further research is needed, as the data quality of Volunteered Geographic Information (VGI) is often low.

5 TOOLS FOR MHRA AND DECISION MAKING

In order to be able to carry out a dynamic multi-hazard risk assessment, several tools are needed for multi-hazard modelling, multi-hazard risk assessment and decision making.

5.1 Tools for Hazard assessment

The landslide hazard assessment methods that can be used as a basis for a dynamic multi-hazard risk assessment have a number of requirements:

- Mass movements are a container terms involving many different processes, and it is very difficult to incorporate them within a single model (e.g. rockfall and deep-seated landslides).
- Separate models have been developed in terms of movement mechanism, initiation, transport, entrainment, accumulation, triggering mechanism

and contributing factors. Models should be integrated in order to simulate the interactions between the processes.

- Spatial risk assessment methods for administrative units require spatial distributed intensity characteristics, which may differ per hazard type (e.g. impact pressure, displacement velocity, volume).
- Hazard models should allow the simulation of hazardous processes at a regional scale. This has implications with respect to the type of models, making it difficult for example to apply detailed limit-equilibrium models or finite-element-models that are used at slope-scale.
- Parameterization of models should be relatively simple, but it is very difficult to obtain sufficient samples on many detailed hydrological and geotechnical properties of soil and rock masses over large areas.
- Models should be able to simulate the chain-interactions between different types of hazardous events.
- Models should incorporate the uncertainty in the input data, and hazard interactions. Also it should be possible to evaluate the sensitivity of the models to the input data in a time efficient manner.
- It should be possible to calibrate the models based on relatively simple to obtain information for specific points.
- Models should be able to simulate changes in triggering factors, and landslide contributing factors.

Statistical approaches for multi-landslide hazard assessment are not considered optimal as input for dynamic risk assessment, since they generally do not provide information on landslide intensities, and depend on historical landslide occurrences, that may have occurred under different conditions than the ones that are there now, or that may occur in future. They are therefore unsuitable for scenario modelling. They also do not allow for modelling initiation and runout behavior in an integrated manner. Although empirical runout models such as Flow-R (Horton et al., 2013) have proven to be useful in multi-hazard risk assessment, as a proxy to physically-based models (Chen et al., 2016).

Spatial-temporal numerical modelling has proven to be one of the best approaches for modelling hazard interactions. Physically-based models are generally able to provide more insight into the underlying causes of hazardous processes and how physical

parameters affect their behavior. Table 1 gives examples of physically-based models for landslide hazard interactions.

In the past decade, there has been a rapid development in physically-based models due to the improved data availability and quality and increasing computational power, that allowed:

- incorporating earthquake triggers,
- including both wetting front and rising groundwater triggers,
- model rainfall-runoff, channel flow and inundation in an integrated manner,
- the development of regional scale landslide failure surface models,
- improved integration of landslide initiation and runout modelling,
- development of flow models with various rheologies,
- incorporation of entrainment,
- Integrated landslide, wave modelling and breach modelling for lake breakout flooding

This led to the development of integrated physically-based multi-hazard models that are capable of simulating all relevant interacting hazard processes, in which mass movements play a role. Three of the most promising models are STEP-TRAMM (Cohen et al., 2009; Von Ruetten et al., 2013; Fan et al., 2017), r.avaflow (Mergili et al., 2017a; 2017b; 2018) and OpenLISEM Hazard (Bout et al., 2018).

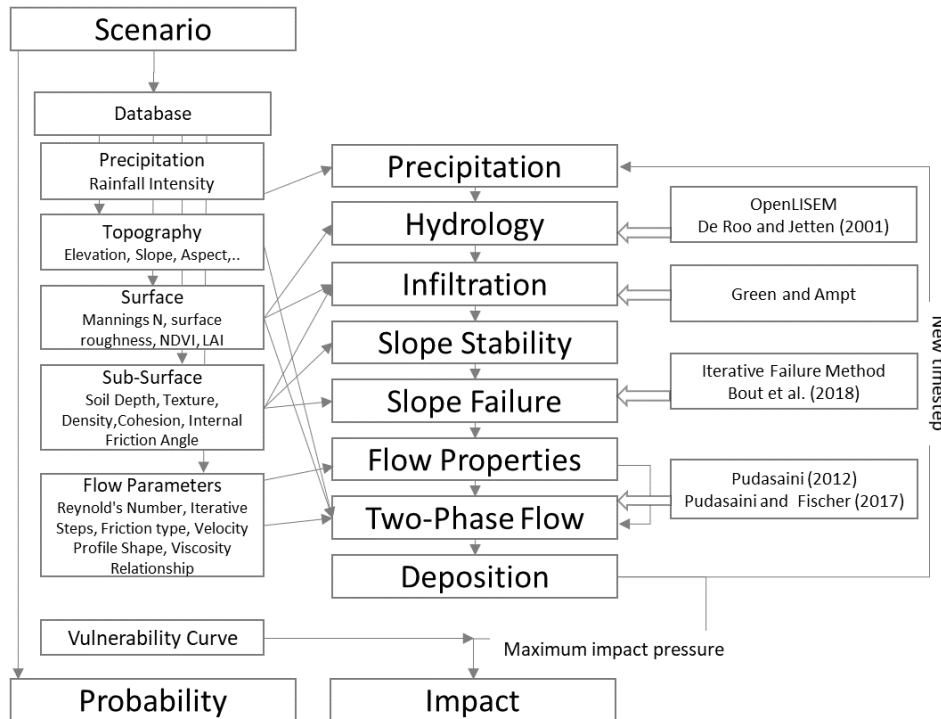
Table 1. Examples of physically-based models for landslide interaction modeling

| Hazard Interactions | Examples of available regional models |
|---|---|
| Modelling slope hydrology and slope stability | TRIGRS (Baum et al., 2002) PROBSTAB+STARWARS(van Beek and Van Asch, 2004) CHASM (Anderson et al., 2008) iCRESTRIGRS (Zhang et al., 2016), SIMTOP (Lee & Ho, 2009) CAPRA Landslide Tool (Hurtado, 2018) |
| Seismic and landslide | SpecFem3D (Komatitsch et al., 2010) CAPRA Landslide Tool (Hurtado, 2018) OpenLISEM Hazard (Bout et al., 2018) |
| Slope Failure Surface | Scoops3D (Reid et al., 2015), r.slope.stability (Mergili et al., 2014) |
| Runout of several types of mass movements | r.avaflow (Mergili et al., 2017), RAMMS (Christen et al., 2010) EDDA (Chen & Zhang, 2015) Flo-2D (O'Brien et al., 1993), |

| | |
|---|---|
| Landslide, River dams, Break out floods | BREACH +SOBEK (Fan et al., 2012) BASEMENT+RAMMS (Byers et al., 2018) RAMMS + FL-2D (Mergili et al., 2011) AUT16+DAM10 (Clerici&Perego,2000) NWS DAMBRK (Alford, 2000) |
| Integrated multi-hazard models | Step-Tramm (Fan et al., 2017) OpenLISEM Hazard (Bout et al., 2018) |

time step for specific rainstorm events. The OpenLISEM tool can be used for both forecasting and assessing the hazard and risk of multi-hazards related to hydro-meteorological extremes. The application of these integrated models is still challenging, as they require relatively many parameters, which are also dynamic in a changing landscape. For example, the topography, soil water

Figure 4: General flowchart for the integrated physically-based multi-hazard model OpenLISEM (Bout et al., 2018)



OpenLISEM is an event-based model that simulates the processes in a catchment as a response to a particular rainfall event. Figure 4 gives an example of the modelling framework of OpenLISEM Hazard, which was originally developed as a hydrology, runoff and erosion model. Later, flash flood behavior was included and in the past years, the model has been updated to include interactions between rainfall runoff processes, slope stability, slope failure, sediment and water mixture, entrainment and deposits. Catchment-scale hydrology directly causes flooding, and influences slope stability, failure and runoff. The integration of hazardous processes in such a setting improves accuracy and allows for a more detailed simulation of multi-hazard events. Slope failure is automatically estimated from instabilities, and shallow landslides are introduced in the flow, where they interact with water flow based on two-phase generalized debris flow equations. Input data related to topography, soils, vegetation and land use are provided as raster data. Rainfall data is given per

conditions, vegetation characteristics, and soil material quantities and characteristics change over time. A major hazardous event will alter the characteristics of the landscape, and the model parameters for the integrated model also change. The use of integrated physically-based multi hazard models allows to re-analyze the hazards, whenever the landscape conditions change as a result of long term, or short-term activities or processes. They are an essential component of dynamic multi-hazard risk assessment for local and regional decision-making.

5.2 Tools for vulnerability and risk assessment

Next to multi-hazard models, it is also important to incorporate multi-hazard vulnerability models, which allow the integration of vulnerability curves for different hazard types. One of the most useful developments in this field has been the development of the ERN-Vulnerability tool, for the creation and edition of vulnerability curves, for different structural types and different hazard intensity types (CAPRA, 2020). It contains a database of available

curves. Unfortunately, curves for landslides are very limited in this tool. Given the large range of landslide processes and intensity types, the best results have been achieved in the development of vulnerability curves (Uzielli et al., 2008), matrices and indices for debris flows (Papathoma-Köhle et al., 2017) and slow moving landslides (Peduto et al., 2017).

The analysis of risk requires a repetitive procedure which has to be carried out for each hazard event (different hazard types and return periods) in combination with elements-at-risk types, and then also for each possible planning alternative. This requires the use of automated procedures and tools that link with Geographic Information Systems. Risk assessment is computationally intensive. It can be carried out using conventional GIS systems, although it is advisable to use specific software tools. Unfortunately most of these catastrophe models are not publicly available, as the risk assessment is carried out by private companies. Newman et al. (2017) provide a review of decision support systems for disaster risk reduction

The earliest and most constant among the publicly available loss estimation tools has been HAZUS developed by the Federal Emergency Management Agency (FEMA) together with the National Institute of Building Sciences (Schneider and Schauer, 2006). HAZUS was developed as a software tool under ArcGIS, and deals with floods, earthquakes and windstorms and associated hazard relations. The loss analysis includes physical damage to buildings with different use, economic loss (lost jobs, business interruptions reconstruction costs etc.) and social impacts (shelter requirements, displaced households, population exposed to hazards). Earthquake-induced landslide susceptibility is applied to site specific structures, and an average landslide susceptibility value is assigned to each census tract, with relative classes ranging from 0 to 10.

One of the most comprehensive attempts to provide open models for quantitative multi-hazard risk assessment is the CAPRA Probabilistic Risk Assessment Platform (CAPRA, 2020) which was supported by the World Bank, and which has also been used in the generation of the global risk assessments for the Global Risk Assessment Data Platform (GAR, 2015). The methodology focuses on the development of probabilistic hazard assessment modules, for earthquakes, hurricanes, extreme rainfall, and volcanic hazards, and the hazards triggered by them, such as flooding, windstorms, landslides and tsunamis. Landslide hazard is analyzed using an infinite slope model, with input

for seismic acceleration and soil moisture (Hurtado and Yamin, 2018). The resulting vulnerability curve is related to the factor of safety, which may not be the most appropriate intensity parameter. Runout is not taken into account.

The OpenQuake tool of the Global Earthquake Initiative (GEM, 2020), is a comprehensive open tool for Probabilistic Seismic Hazard and Risk Analysis. It does not contain an earthquake-induced landslide component yet.

The RiskScape tool, which has been developed in New Zealand (Reese et al., 2007; Schmidt et al., 2011), is a generic toolbox for the integration of hazard, assets and vulnerability functions. It can be connected with a number of different hazard models, which provide the required hazard information. The system does not allow modelling the interaction between multiple hazards and assets in a risk scenario, but plans are there to implement this, for example for earthquake-induced landslides. Currently the system only contains the options to analyse landslide exposure. The next general release that contains also a probabilistic component is expected in mid-2020.

There have been a variety of successful studies that link meteorological hazards to impacts. An example of this is the open-source software CLIMADA (CLIMate ADaptation) (Aznar-Siguan and Breach, 2019), which integrates hazard, exposure, and vulnerability to compute the necessary metrics to assess risk and to quantify socio-economic impact of hurricane-related hazards at a general scale. It does not contain a landslide component.

5.2.1 RiskChanges SDSS

Within the framework of the EU FP7 Marie Curie Project CHANGES (www.changes-itn.eu) and the EU FP7 Copernicus project INCREO a spatial decision support system was developed with the aim to analyze the effect of risk reduction planning alternatives on reducing the risk now and in the future, and support decision makers in selecting the best alternatives. The Spatial Decision Support System is composed of a number of integrated components (Figure 5). The Risk Assessment component allows to carry out spatial risk analysis, with different degrees of complexity, ranging from simple exposure (overlay of hazard and assets maps) to quantitative analysis (using different hazard types, temporal scenarios and vulnerability curves) resulting into risk curves. The platform does not include a component to calculate hazard maps, and existing hazard maps are used as input data for the

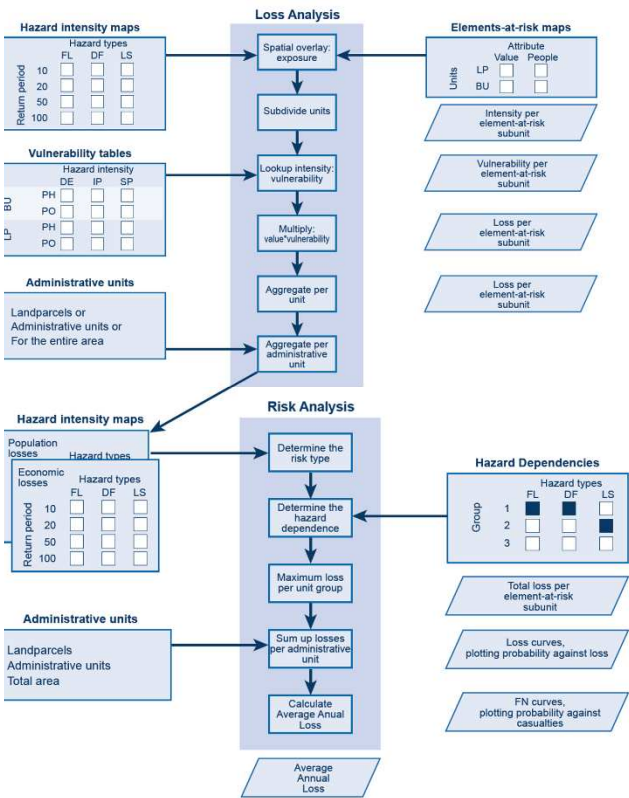
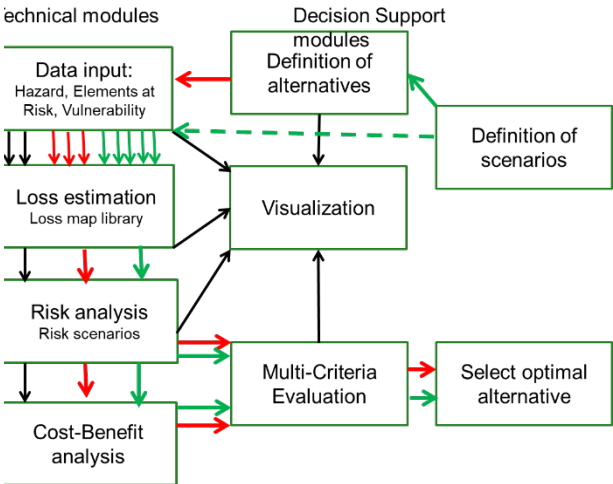
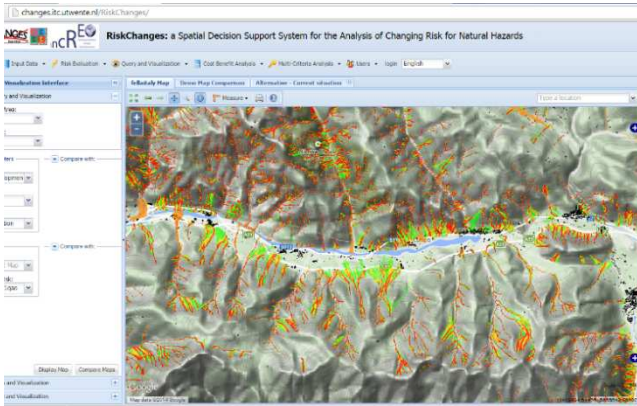


Figure 5: Above: User interface of the RiskChanges SDSS. Middle: Modular structure of the SDSS. Below: Loss and Risk Assessment procedure used.

risk component. The second component of the SDS is a risk reduction planning component, which forms the core of the platform. This component includes the definition of risk reduction alternatives (related to disaster response spatial

planning) and links back to the risk assessment module to calculate the new level of risk if the measure is implemented, and a cost-benefit (or cost-effectiveness/ Spatial Multi Criteria Evaluation) component to compare the alternatives and decision making. The third component of the SDSS is a temporal scenario component, which allows to define future scenarios in terms of climate change, land use change and population change, and the time periods for which these scenarios will be made. The component does not generate these scenarios but uses input maps for the effect of the scenarios on the hazard and assets maps. The last component is a communication and visualization component, which can compare scenarios and alternatives, not only in the form of maps, but also in other forms (risk curves, tables, graphs). The envisaged users of the platform are organizations involved in planning of risk reduction measures, and that have staff capable of visualizing and analyzing spatial data at a municipal scale. The Decision Support System RiskChanges is accessible at: <http://sdss.geoinfo.ait.ac.th/> and examples at Van Westen (2014) and http://www.charim.net/use_case/46

6 CASE STUDY ON MHRA FOR ANALYSING CHANGING RISK

To illustrate the application of integrated physically-based multi-hazard models for the analysis of changing risk, an example is shown from the Colombian city of Envigado (Figure 6). Envigado is one of the ten municipalities within greater Medellin, located along the Aburra valley, underlain by metamorphic rocks that have altered by past tectonic activity, weathering and denudational processes producing extensive slope deposits and frequent landslides (Hermelin, 1984).

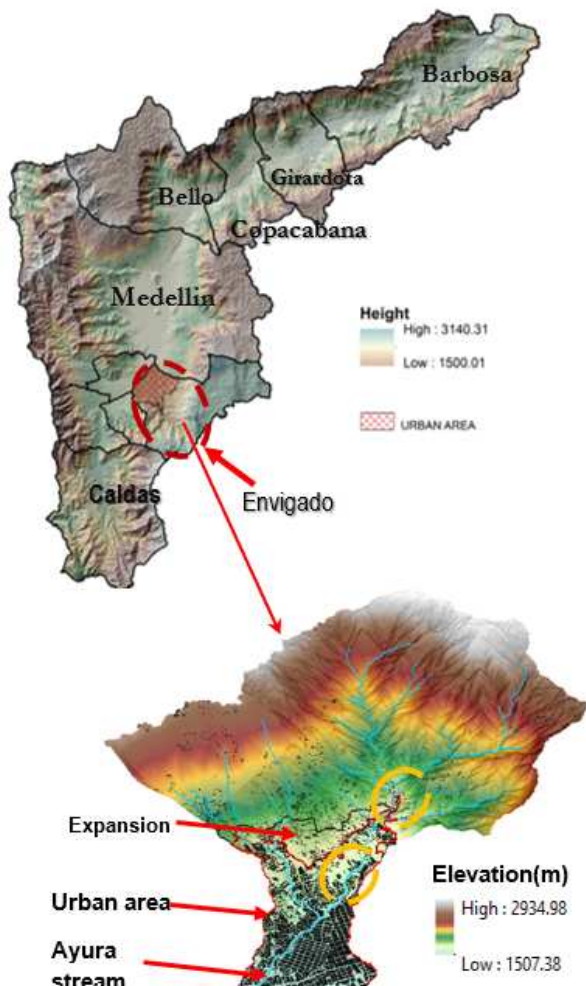
Landslides are triggered by earthquakes and rainfall. Recent earthquake-induced landslides have not occurred, but geomorphological analysis of old landslides point out that many may have been caused by earthquakes in the past (Garcia, 2006). Aristizabal et al. (2011; 2016) have analyzed the antecedent rainfall and established rainfall thresholds.

Hazard and risk studies were carried out by the National University of Colombia and the local government of Aburra Valley (AMVA, 2018). These studies are part of efforts that date from the '90s in the region (Coupé, 2011) and that currently count with the input of real-time monitoring of environmental variables proceeding from important local risk management projects such as SIATA

strengthen recently by important initiatives such as 100 Resilient Cities (2019). The studies focused on mass movements, flooding and other flow-like phenomena (debris flows) which are a threat to the municipalities within Aburra Valley that are mostly situated on alluvial fans.

Envigado is located south of the municipality of Medellin. It has an area of 79 km² with elevation ranging from 1550-2900 m.a.s.l. The urban center is located in the lowest zone and has an area 12.2 km². Extreme events of flood and debris flow occurred in the years 1938, 1944, 1950 and 1988. There is very limited information available about the impacted area and causal factors available, due to the rapid growth of the city, from a small village in 1943 to a city with an estimated population of 220 thousand inhabitants in 2016. The event from 1988 was triggered by landslides in the upper watershed that combined with the stream flow of the main drainage of the city, the Ayura stream, into a debris flow and flashflood event (Caballero, 1988 and Florez & Parra, 1988). It is important to know how a new event would affect the city, which is now much

Figure 6: Location of the case study of the Ayura watershed, in the city of Envigado, one of the municipalities of greater Medellin in the Aburra valley.



larger than in 1988 when the last event occurred. As a result, different hazard analysis projects have been performed (AMVA, 2018).

6.1 Method and input data

The aim of the study was to analyze the changing multi-hazard risk within the city of Envigado, resulting from a combination of landslides, flashfloods and debrisflows in the Ayura Stream. This was done by comparing the present level of risk with that of possible future changes, resulting from scenarios with a combination of urban growth and climate change for the year 2050. A number of risk reduction alternatives was also evaluated in order to analyze which one of these would have the largest risk reduction. Figure 7 gives a flowchart of the procedure. Table 2 gives a summary of the input data.

Table 2. Input Data for MHRA in Envigado

| Type | Source | Date |
|---|-----------------------------------|------|
| Lithology and soils | AMVA(2018) | 2018 |
| DTM with 2 m resolution | IGAC | 2014 |
| Event Inventory | DesInventar | 2018 |
| Landcover. Image classification | AMVA(2018) | 2018 |
| Rainfall data. IDF curves | AMVA(2018) | 2018 |
| Hazard footprints produced by AMVA with IBER 2D software (RP=500y) and HEC-RAS (RP=25,50,100 y) | AMVA(2018) | 2018 |
| Seismic information. Peak ground acceleration map 10% exceedance probability in 475 years | Universidad de los Andes, 2015 | 2016 |
| Land use | Master plan (POT,2011) | 2011 |
| Building footprint from 2011 updated for present situation | Master plan (POT,2011) | 2017 |
| Road Footprint | Master plan (POT,2011) (POT,2011) | 2011 |
| Population data | No data | - |
| Value of buildings | AMVA(2006) | 2006 |
| Vulnerability curves | Ciurean (2017) and CAPRA (2020) | - |

6.2 Analyzing current risk level

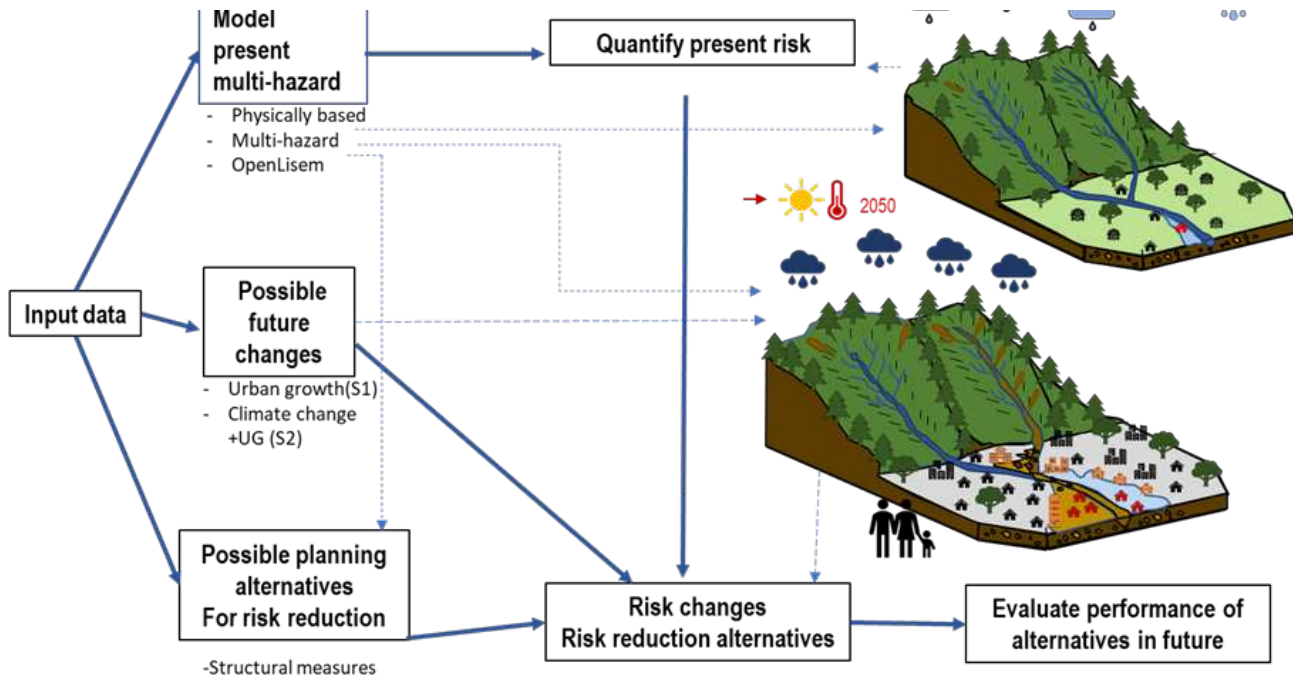
In order to analyze the current level of risk the risk components of hazards, elements-at-risk and physical vulnerability were prepared.

6.2.1 Hazard modelling

Hazard maps for flooding and debris flow/hyper-concentrated flows were produced for the present situation of the Ayura watershed using the

OpenLISEM Hazard model (Bout et al., 2018, See Figure 4). The model requires the following input maps:

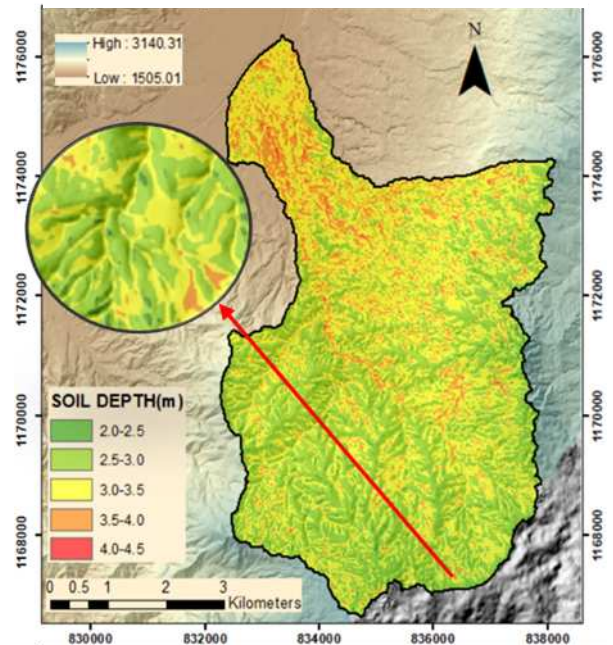
Figure 7: Procedure for the analysis of future risk changes in the municipality of Envigado, Aburra Valley, Colombia



- Topography.** The available DTM with 2 m resolution was resampled to 5 m, as otherwise the dataset would be too computationally intensive. Some bridges had very low slabs inside the river channel resulting in a reduction of the hydraulic capacity of the stream. To represent this effect, the channel depth was uplifted at bridge locations.
- Soil properties.** Important soil parameters such as parameters evaluated were cohesion (c'), effective internal friction angle (ϕ') and density (γ) were obtained from AMVA (2018). Other parameters such as hydraulic conductivity (k_{sat}), medium grain size (D_{50}), porosity (θ_s), initial moisture content (θ_i), residual moisture content (θ_r), and average suction at the wetting front (ψ_i) were estimated using literature and reports from earlier studies in Envigado, a compendium of soil properties (Koliiji, 2008) and using pedo-transfer functions.
- Soil depth.** A soil depth map was produced (Figure 8) based on the methods by Kuriakose et al., (2009) and Von Ruetten et al., (2013). While Kuriakose et al., (2009) used topographical factors to define soil depth, Von Ruetten et al., (2013) used

soil production and transport balance assuming that topography is at steady-state.

Figure 8: Soil depth map for Ayura watershed



d cover map produced by AMVA (2018) was modified based on visual image interpretation. Surface roughness (Manning's n) values were assigned to each landcover class. Maximum canopy

storage was calculated based on Jong and Jetten (2007), based on NDVI and Leaf Area Index (LAI).

- Precipitation data.** Different rainfall events with 25, 50, 100, and 200 years return period were designed to evaluate the response of the watershed. These were constructed using IDF curves produced by AMVA (2018) who used the data of one station in the area. These IDF curves were developed using a Gumbel analysis with data from the year 1996 to 2016 with 15 minutes resolution. From the IDF curves, synthetic rainfall events were created, using the alternating block method for a time of 170 minutes. This time corresponds to the concentration-time of the watershed calculated by AMVA (2018). One example is shown alongside the IDF curves in figure 9.
- Antecedent rainfall conditions.** As OpenLISEM is an event-based model, the simulation of antecedent conditions such as groundwater variations resulting from antecedent rainfall, was carried using a separate model that worked with a time-step of 1 day. This model increased the initial soil moisture (θ_i) with values ranging from 7% to maximum values of 50% in concave areas near the river

course.

Calibration of the model was based on the flooding results of AMVA (2018) for the return period of 25 years. Validation was based on the limited available data for the landslide locations and the flood extend reported in specific locations during the 1988 event.

Flood and debris flow intensity was modelled for the return periods of 25, 50, 100 and 200 years. Maps were generated of maximum flood height and maximum debris/hyper-concentrated flow height for each return period. Figure 10 gives some examples of the output maps.

6.2.2 Elements-at-risk database

The Planning Office of Envigado provided an updated building footprint database based on the elaborated for the Master plan of Envigado (POT, 2011). However, this digital building footprint map contained a large number of topological errors, and including many small polygons (e.g., elevator spaces, terraces etc.) which were not buildings. These issues were manually corrected using GIS to guarantee that each polygon represented a building unit. Buildings were classified in the following classes: residential (R), commercial (C), educational (E), health care (H) and industrial (I). Other building attributes, e.g. on construction type, were not available, so we assumed a relation between the building height and construction type. Buildings were classified into three main groups (See Figure 11).

Building costs were retrieved from an earlier study on seismic micro zonation of the Abura Valley (AMVA, 2006), which presented unit costs per m^2 for R, C, I uses. An update of the prices was made using the inflation rate and the consumer price index (IPC) for the last 2 decades in Colombia (an increase of 4.9% per year). The market costs per land use in 2018 were considered for residential 630.9 €/m^2 , for commercial 775 €/m^2 and for industrial 725 €/m^2 .

The only detailed source of population information was a report (Alcaldía de Envigado, 2018) with an estimation of the population by neighborhood within the municipality of Envigado based on the projections to 2016 of the census in Colombia from 2005. We calculated the population density by neighborhood, by dividing the number of people per neighborhood by the total floor space area of residential buildings (footprint area multiplied by the number of floors).

Figure 9: Above: IDF curves for different return periods (AMVA, 2018). Below: Synthetic rainfall event with 100 Year return period.

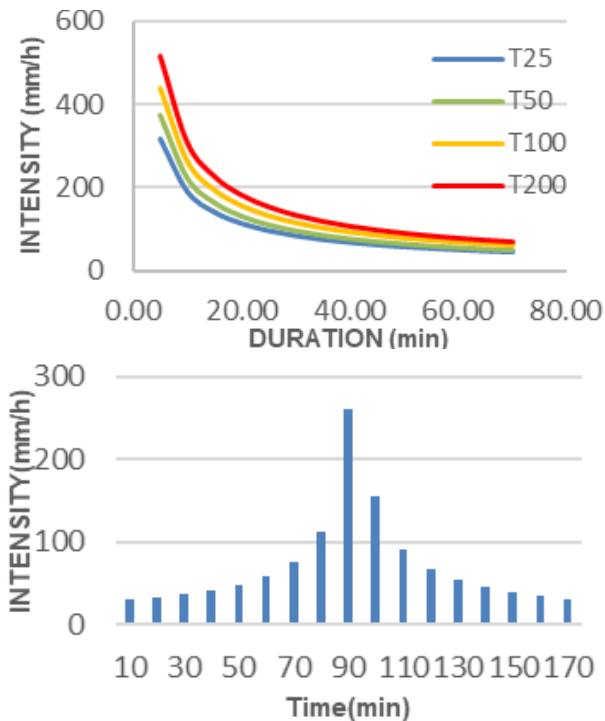
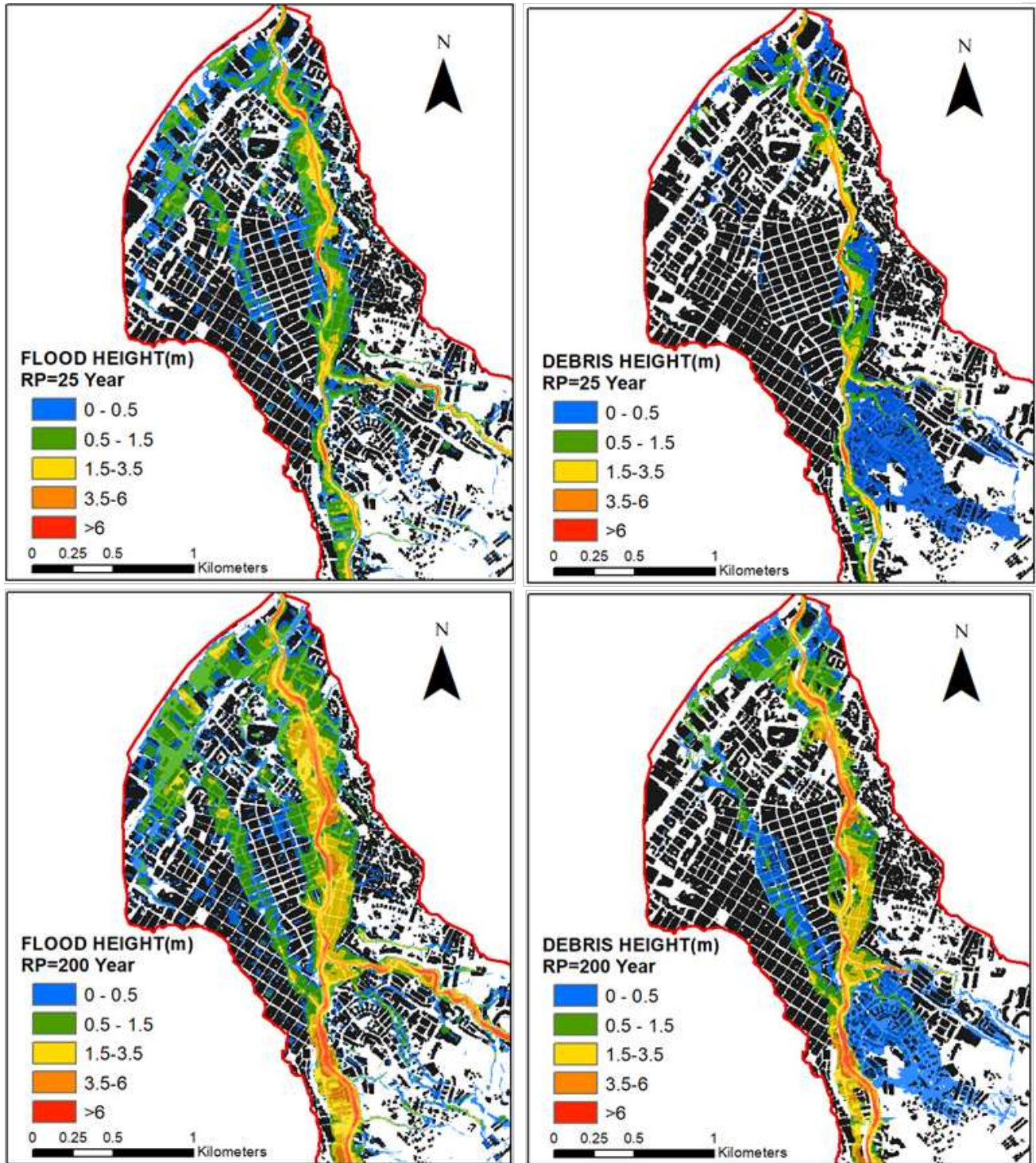



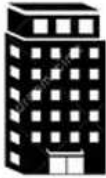
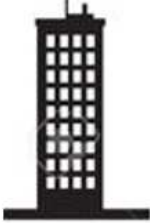
Figure 10: Examples of flood and debris flow intensity maps. Maximum flood height (left) and debris flow height (right) for 25 year (above) and 200 years (below) Return period.



Then to estimate the population inside the catchment of the Ayura stream for each building in the neighborhood, the number of people was calculated by multiplying the density per neighborhood with the total floor space for residential buildings. As a result, from the 219,991 inhabitants reported for the whole of Envigado by 2016, 108,737 inhabitants were estimated to be living inside the study area. A nighttime occupation scenario was taken into account, which was

considered the most critical if a debris flow-like phenomena occur. During the day, a large proportion of the population leaves Envigado to work in the capital of the region, Medellin, and returns home in the evening. For this scenario, it was assumed that the population that stays in the municipality would leave the non-residential areas (e.g. schools, commercial areas, and industrial areas) in the night. For this reason, the possible areas where the population can be located now of a

Figure 11: Characterization of the three building types in the study area

| Low-rise: Single floor buildings | Medium-rise: Two to six floors | High rise: More than six floors |
|--|---|--|
|  |  |  |
| <ul style="list-style-type: none"> • Will sustain structural and non-structural damage during flood & debris flow. • Could be completely destroyed. • Population cannot evacuate to upper floors so are more vulnerable to flood and debris flow. | <ul style="list-style-type: none"> • Will sustain non-structural damage in lower floors. • May have structural damage in lower floors. • Population can escape to upper floors so population risk is very low. | <ul style="list-style-type: none"> • Will only sustain non-structural damage in lower floor. • Very limited structural damage. • Population can escape to upper floors so population risk is very low • Parking garage for residential and commercial buildings, which may be subjected to high damage |

hazardous event might be the residential areas (R) and health care establishments (H). Although Envigado has also a substantial entertainment sector, we did not have enough information to include this in the land use classification and in the nighttime population scenario.

After processing the data to make them usable, a building shapefile of the study area was produced, with attributes on land use, building type, value per floor and number of people per floor.

6.2.3 Physical vulnerability of buildings

It was decided to develop absolute curves instead of relative curves (between 0 and 1), due to the presence of many high-rise buildings, many of which with subterranean garages. The calculation of the loss as the value for the entire building multiplied by the relative physical vulnerability was considered less reliable, than using absolute loss values directly related to depth for the various building types.

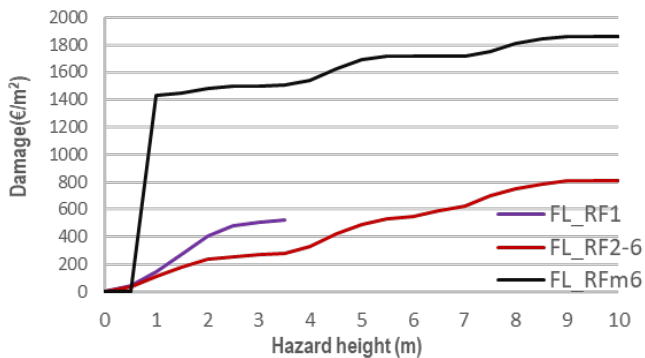
To construct the absolute vulnerability curves four parameters were used: damage to building contents, structural and non-structural building damage (only here relative curves were used as will be explained later), cleaning costs and losses of cars in subterranean garages.

- **Damage to building content**, was calculated by assuming a standard set of possible articles (furniture, equipment etc.) in an apartment with a surface of reference of 100 m² (which is the estimated average space for families of 4-5 people in Colombia. The damage for articles of a single floor and medium-rise buildings was estimated using the approach of van Westen et al., (2014), in relation to the water or debris height.

- **Structural damage to buildings** was estimated using relative vulnerability curves, multiplied with the building cost values. Only 60% of each building value was taken following Bruijn et al., (2014). Relative vulnerability curves for flooding were taken from a database used by CAPRA (2020) in the Latin-American context called ERN-Vulnerability. These curves were for buildings with different structural systems, number of floors, and relate the damage with flooding depth. For debris flows the curves presented by Ciurean (2017), generated from a number of other sources were used. For medium and high-rise buildings, these curves were further adjusted because of the assumed increase in resistance of structural systems for multistory buildings.
- **Clean-up costs** were estimated for flooding and for debris flows. For flooding, rates of 0.57 euros per m² (for water levels between 0 to 1m) and 2.8 euros/m² (for flow heights more than 1m) were used. For debris flow the values were substantially higher (15 €/m³) as they include removing and transporting heavy solid materials (as rocks, structural elements, wood, mud and water). We assumed that all residential and commercial buildings with more than six floors had an underground garage with a height of 3.5 m, which would result in additional cleaning costs. Also it is considered the removal of cars once the flood level outside the building surpassed 1 meter and the garage would be flooded. The losses of vehicles in these flooded garages was also estimated.

Once the costs for building contents, structural and non-structural elements, clean-up and garages contents

Figure 12: Example of an absolute physical vulnerability curve for Flooding of residential buildings RF-1 = low-rise, RF2-6 = Medium-rise, RFm6= high-rise



were estimated per m² they were added. The added value varied in function of the hazard intensity (water and debris flow height). In total 30 absolute vulnerability curves were generated. An example is shown in Figure 12.

6.2.4 Risk modelling

In this study equation [1] was used to calculate the potential losses or risk associated with the multi-hazards. The risk corresponds to the economic risk of buildings, exposed to flooding and debris flow. The risk results are presented as the average annual loss in Euros using the approach of the risk curve. The analysis was implemented in scripts using GIS. A loss calculation was made for every combination of hazard type (flood or debris flow) and return period. For the present situation, this resulted in the calculation of 8 loss scenarios. As flooding or debris flow can occur simultaneously or sequentially during the same event, the maximum damage of either one of them per building is used in calculating the combined risk.

Table 3: Resulting losses for flooding, debris flow and the combination (values in million Euros)

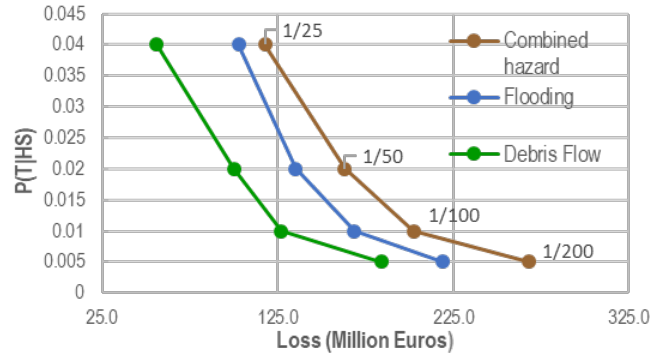
| Return Period | Flooding | Debris flow | Combined |
|---------------|----------|-------------|----------|
| 25 | 103 | 56 | 118 |
| 50 | 136 | 100 | 163 |
| 100 | 169 | 127 | 203 |
| 200 | 219 | 184 | 268 |

To calculate the risk the approach of the loss curves was used. Loss curves plot the temporal probability against the loss for the different scenarios with different frequencies. A curve is fitted through the points. In this curve events of higher magnitude occur with lower frequency and events with low magnitude produce more

frequent losses over time. The area under this curve is known as the average annual economic risk. Figure 13 present the resulting loss curves.

The overall average annual risk is 6.4 million Euros/year (for the present situation). This was compared with the risk for several future scenarios and with the changing risk due to the implementation of possible planning alternatives.

Figure 13: Risk curves for the present situation



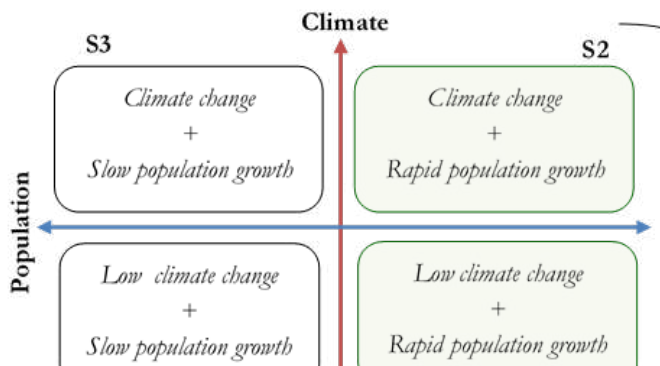
6.3 Analyzing changing risk for future scenarios

Climate change combined with political and economic changes lead to the modification of the temporal patterns of natural hazards and exposure of the elements at risk (CHANGES, 2014). As a consequence, the risk is expected to change considerably which may make it necessary to consider planning alternatives to respond and reduce the risk.

A better knowledge of how the risk will vary can help decision-makers to undertake actions not only for the present situation but as well for future conditions with the maximum benefit for society.

To visualize the possible effects of the economic, population and climate changes the use of scenarios is a solution, which are “plausible pictures of the future”. Scenarios are possible future developments, where current decision makers have limited possibilities in influencing which scenario might develop in reality. They can make decisions on possible risk reduction measures that could be implemented now. In this research, four scenarios for the study area for the future

Figure 14: Four possible future scenarios that were considered in this research



year of 2050 were defined (See Figure 14).

6.3.1 Rapid Population growth

Scenarios S1 and S2 include a rapid population growth within the study area, which will result in an additional pressure on the available residential areas leading to the transformation of certain parts of the city into more dense residential areas with higher buildings. According to DANE (2019) and Horbath (2016), Envigado has an average population growth rate of 2.06% per year based on the number of inhabitants from 1985 to 2016. If this rate of growth is sustained in time, by applying a prediction formula (University of Oregon, 2002) the population in 2050 might increase to 440 thousand inhabitants. However, currently the population pressure is aggravated by the inflow of refugees from Venezuela, and it is estimated that around 10 per cent of an approximate million immigrants from Venezuela have arrived in the Aburra Valley. Most of this incoming population most probably will be settling in four of the most important municipalities of the Aburra Valley (Medellin, Envigado, Itagui and Bello). This might produce a major shift in the population and will result in an additional demand of floor space. Therefore, by projecting to 2050 the population in Envigado might reach 500.000 inhabitants.

To estimate the additional floor space that the new population will require by 2050, we use the minimum required floor space per person, which is 8.75 m² per person (Ministerio de Ambiente Vivienda y Desarrollo Territorial, 2004). This norm applies mainly to the so-called housing of social interest constructed in low socio-economical levels. As the overall economic conditions of the population of Envigado are higher, we used a minimum area per inhabitant of 20 m². Using this in combination with the additional population by 2050 in the study area of 140.000 inhabitants, and additional floorspace of 2.8 million m² would be required.

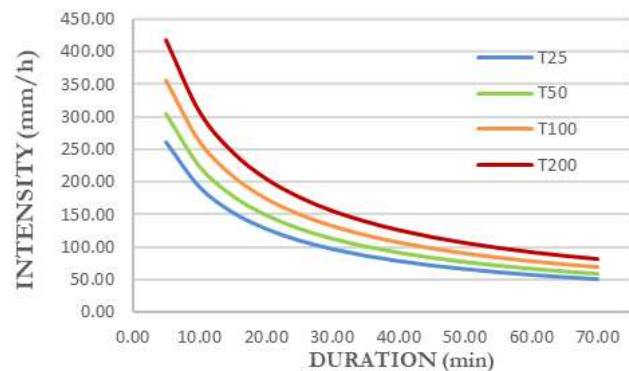
The Master plan of the municipality (POT, 2011) proposed a number of spatial planning guidelines for future land use. These guidelines were interpreted, for the present study, as urban densifications in height and expansions in specific areas. An estimated 70% of the required footprint area (2 million m²) would be located in current residential areas that would be densified, by demolishing the existing ones and constructing taller buildings. Several criteria were used to identify areas that would be suitable for densification: existing buildings with 3 or less floors, and spaces with a minimum surface area of 100 m². The additional 30% of the required floor space in 2050 (0.8 million m²) should come from new expansion areas (nearby to the already urbanized areas). The type of construction will be multifamily apartment buildings with height ranging

between 8 to 16 floors (POT, 2011). In this way, 899 existing residential buildings were selected to be replaced by taller buildings, and 337 new buildings would be constructed to accommodate the incoming population. Based on this, a building footprint scenario map for 2050 was generated, and the building types were adjusted. It is clear that there will be more high-rise buildings in 2050 than there are now, and this would have consequences with respect to the building costs, population density and physical vulnerability.

6.3.2 Climate change effects

The special report on extremes (SREX), published by the IPCC (2012), highlights that the frequency of heavy precipitation will likely increase in the current century. More frequent intense rainfall will affect directly the production of shallow landslides and flow-like phenomena with solid phase, while increases in total

Figure 15: Adjusted IDF curves taking into account climate change for 2050 (AMVA, 2018)

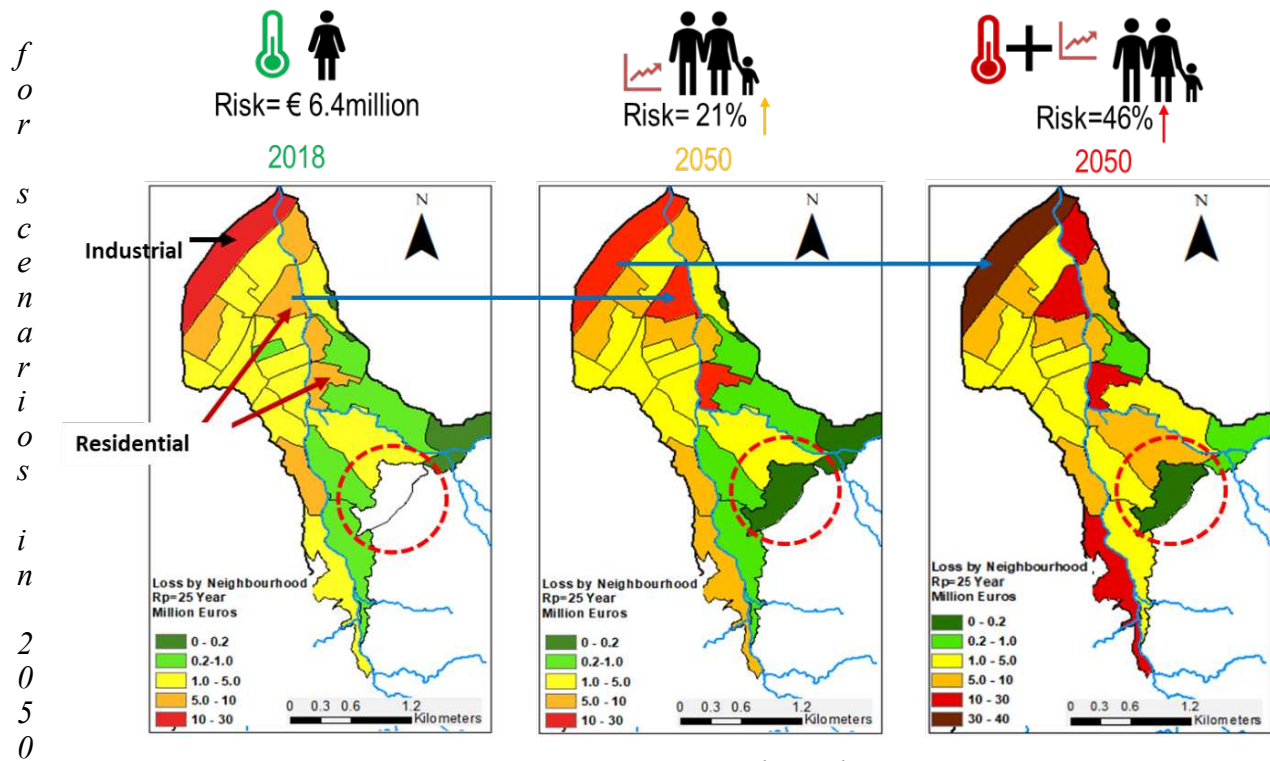


rainfall will influence the detonation of deep-seated landslides (Gariano & Guzzetti, 2016). Climate change can result in more frequent high intensity rainfall. In this way, to represent modifications in precipitation the rainfall was increased for each of the return periods used to model the hazard of the present situation or 2018. To do that, the IDF curves for 2018 were modified, projecting them to 2050.

AMVA (2018) projected the present IDF for a 100 years period, by multiplying the rainfall intensity of the 99 percentile with a growth rate. This rate was found using an analysis of the historical precipitation from 1996 to 2016 in the different catchments of the Aburra Valley. According to AMVA (2018), these projections are valid for rains of short duration (less than 3 hours), so they affect mainly the rainfall intensity. The adjusted IDF curves for 2050 produced by AMVA (2018) are shown in Figure 15. The regional increase of precipitation following RCP 8.5 (2040-2070) was estimated to be between 10 and 20% (Armenta et. al., 2014)

6.3.3 P

Figure 16: Comparing the AAL for 2018 with the expected AAL in 2050 using scenarios of population change (middle) and a combination of population change and climate change (right)



The new hazard situation with climate change was modelled with OpenLISEM for the return periods of 25, 50, 100 and 200 years. A series of eight new maps were produced for debris flow and flooding for the year 2050. Figure 16 shows the percentage of change between the risk in 2018 and 2050 for the scenarios S1 and S2. Flooding and debris flow might increase in height between 20-50 per cent by 2050. This, in combination with the increased value of the exposed elements-at-risk, will result in an increase in risk by 2050, which ranges between 21% (for S1, which only includes population growth) and 46% (for S2, which also includes climate change).

6.4 Risk reduction alternatives

In order to reduce the risk to flooding and debrisflow in Envigado a range of risk reduction alternatives could be considered, which may be range from construction engineering works to relocation of high-risk buildings, and implementing early warning systems. Several interventions in the area have already been carried out to reduce the risk, such as the construction of a concrete channel along the stream, slope stabilization and erosion control works in the upper catchment and restrictive zoning. Therefore, additional risk reduction measures were considered to strengthen or complement the existing ones in order to improve the hydraulic capacity of the existing channel, the capture of sediments and to reduce the vulnerability of buildings.

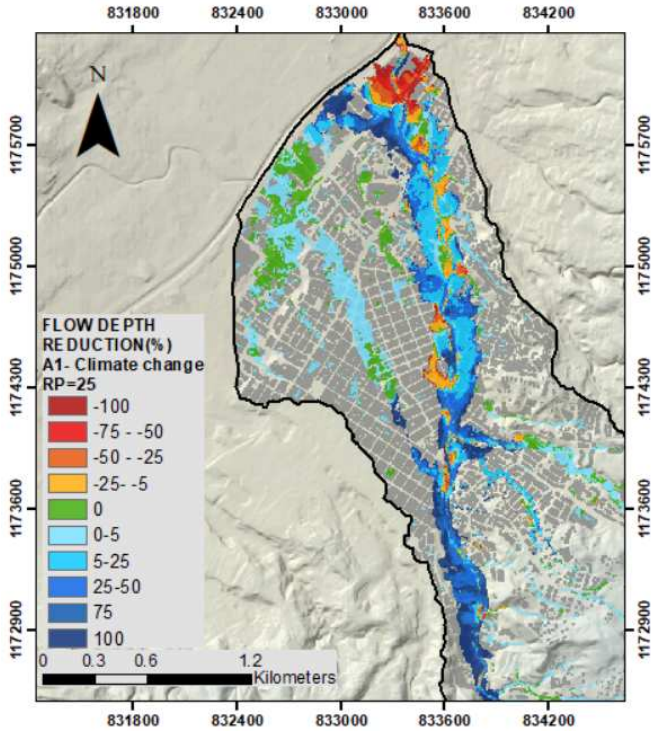
6.4.1 Channel interventions

One of the obvious risk reduction alternatives was to improve the hydraulic capacity of the Ayura stream, by the removal of obstacles and the cleaning of the channelized sections. Existing obstacles such as low bridges were removed and the overall channel cross sectional area increased. A new rectangular channel with dimensions of 15m wide and 5m deep was introduced in the DTM. The goal of this was to improve the water flow in proximity to the main Hospital of Envigado and reduce flooding. To simulate the cleaning of the channel the roughness of the channel was altered by reducing the Manning’s n values. For this alternative, the existent concrete channel was also expanded upstream with 1.2 km. Once the DTM was modified to place the improved channel, OpenLISEM modelling was carried out with the new set-up. Figure 17 gives an example of the change in flow depth resulting from the channel intervention.

6.4.2 Sediment retention measures

The mitigation of debris flows through the stabilization of the source areas might be less effective than the implementation of sediment retention structures along the stream, because stabilization would need to be implemented in the entire source area, which may be large. Given that the historical occurrence of destructive debris flow in the watershed is not very high sediment retention structures can be implemented without

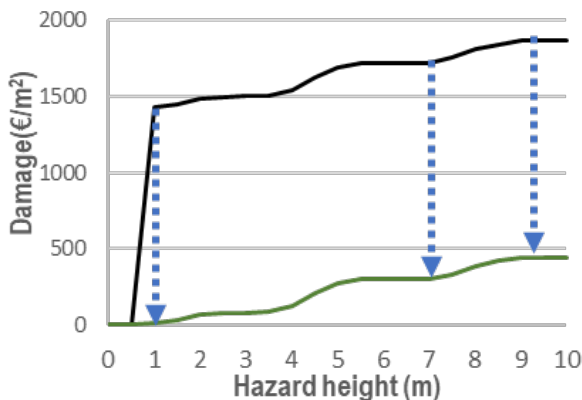
Figure 17: Reduction in flow depth resulting from the implementation of canal improvement and removal of obstructions



incurring in highly recurrent maintenance or replacement (considering the common lifespan of civil engineering works) that could make these projects less feasible. A package of solutions intended to reduce shallow landslides occurrence and to capture sediments was proposed as the second risk reduction alternative. We assumed that if this package of solutions performs successfully, it would eliminate the occurrence of debris flows. Therefore, only flood maps and no debris flow intensity maps were used to model the risk for this alternative.

6.4.3 Protection of parking garages

Figure 18: Adjusting the vulnerability curve for high-rise buildings, to incorporate the protective effect of gates for the parking garages



This alternative was not focused on modification of the hazard, but involved interventions with floodgates to

protect the underground garages in high-rise buildings, which are responsible for a substantial loss during a flood or debris flow event. The protective doors could seal the underground parking garages completely, avoiding the entrance of water and debris. In the calculation of the risk for this alternative, the hazard was not modified. Instead, the absolute vulnerability curves were modified removing the damages of vehicles and the cleaning of the underground garages (see Figure 18).

6.5 Analyzing changing risk

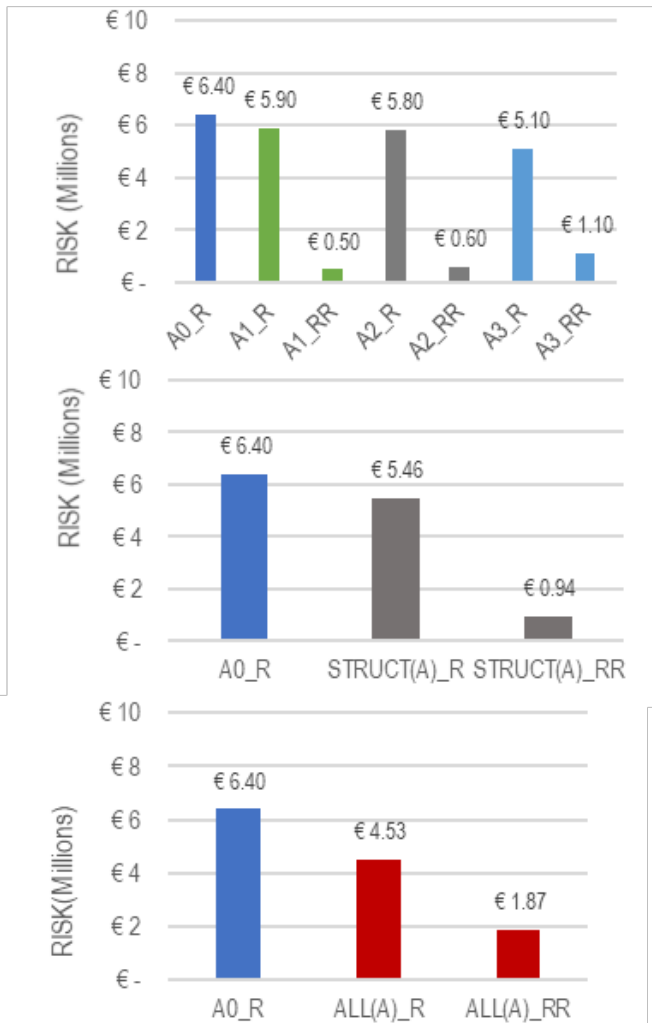
To reduce the risk the alternatives A1, A2 and A3 were implemented. Three combinations of the alternatives were explored: risk reduction (in Euros) for the implementation of individual alternatives, risk reduction for the combination of alternatives for hazard reduction (A1+A2,) and the risk reduction for the combination of the 3 alternatives (A1+A2+A3 or ALL).

The effect of Alternative 3 (flood protection of parking garages) results in a much larger risk reduction than the two structural mitigation measures. If all alternatives are combined, it results in a risk reduction of about 30%.

In order to analyze the behavior of the risk reduction alternatives in future, they were analyzed under the two probable scenarios (population change, S1, and population change combined with climate change, S2). Figure 20 present the resulting risk curves for the combination of alternatives and scenarios.

As it can be seen in Figure 20, the introduction of the alternatives produced a substantial reduction in losses, in such a way that the expected losses in 2050 are less than those for the present situation (S0). The individual effect of the risk reduction alternatives for the two future scenarios is shown in Figure 19. The effect of risk alternative A3 is such that it slightly reduces the risk in future or results in a small increase, which is different for the two others, which have a relatively small effect in reducing the risk. The highest risk reduction by itself is not sufficient to select the best alternative since different constraints can play a role, which could be related to environmental, economic, political or social implications. In order to evaluate the relation between the investment and benefits involved for implementation the risk reduction alternative, the maintenance costs to keep it functional, and the risk reduction it will achieve, it is important to carry out a cost-benefit analysis (CBA). Investment costs were estimated for the risk reduction alternatives, and the time that would be required to carry out the implementation. As a result, the maximum investment that would be required to maintain the profitability of the risk reduction alternatives was 20.8 million euros.

implementation of the risk reduction alternatives. Above: the risk (R) and risk reduction (RR) of the three alternatives separately. Middle: the risk R and risk reduction of the structural mitigation measures (A1+A2). Below: the risk R and risk reduction of the combination of alternatives (ALL). All values in million Euro.



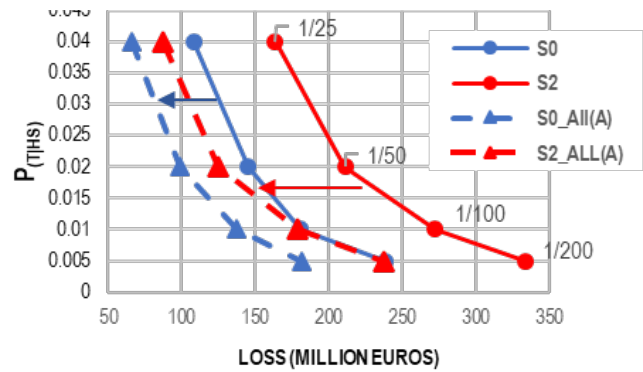
Other factors that determine the selection of the best risk reduction alternative may not be expressed in monetary values but indicate the preference of a specific stakeholder groups (e.g. municipal authorities, affected population, commercial sector). The identification of the indicators that are used in the selection, and the assignment of relative priorities to these can be carried out using Spatial-Multi Criteria Evaluation.

7 CONCLUSIONS

The analysis of static landslide risk has been a challenge (Van Westen et al., 2006) for a long time, and was considered complicated due to a range of factors, related to the high spatial variability and uncertainty of the causal factors and the difficulty to model them over larger areas, the lack of sufficient historical and spatially referenced landslide inventories, and the difficulty to model intensity maps, and link these with appropriate vulnerability curves.

SLIDES

the situation in 2050 following scenario S2, and the effect of all risk reduction alternatives combined for the present situation (S0_ALL(A)) and for scenario 2 (S2_ALL(A))



Landslide hazard assessment is by definition a multi-hazard assessment, due to the large variety of landslide processes, and the way they interact. Also because landslides are very often part of hazard interactions with other geological or hydro-meteorological processes that require to analyze landslides as a consequence of another process. Linked to that is the difficulty to analyze magnitude-frequency relationships of landslide processes by studying the occurrence of the processes by themselves. This is due to lack of historical data, and the fact that they mostly do not happen on the same location repeatedly, with the exception of processes like rockfall or debris flows, and if they do, they modify the terrain conditions, affecting the likelihood of new occurrence. Therefore most landslide hazard and risk studies need to make use of magnitude-frequency relationships of triggering events (such as rainfall and earthquake) which have to be translated to slope stability through additional soil moisture and topographic /soil seismic amplification modelling.

Major achievements to address these challenges in analyzing landslide risk have been the wide use of satellite data (for landslide inventory mapping, monitoring of slow moving landslides, precipitation) and their use in development of global datasets (topography, geology, land cover, soil characteristics, buildings and roads), collaborative mapping (e.g. landslide inventory mapping, earthquake intensity, OpenStreetMap), and the enormous increase in computing speed, allowing the use of more sophisticated models over large areas.

The development of integrated physically-based multi-hazard models within an operational context is now within reach. Whereas previously separate models were used for individual processes, and the link between one model and the next was always problematic, the processes and their interactions can now be modelled in the same tool.

However, the application of such models in multi-hazard risk assessment studies is still faced with serious challenges.

- The first one is related to the large number of input parameters that are required. Some of the models require over 15 spatial varying parameters, which can, at best, only be measured for a few locations, and otherwise are modelled as proxies from other factors. Sensitivity tests have shown which parameters are most influencing the output. Soil depth, for example, is a very important factor, and several soil depth modeling approaches that have been applied show promising results.
- The difficulty in calibrating and validating the models. Models can be calibrated for measured discharge or soil moisture changes at specific locations, or can be validated for the extend of landslides and runout for historical events. However, the calibration might often lead to a situation where, after tweaking the model parameters, the model can reproduce the pattern of a historical events well but behaves poorly in similar nearby areas, or for other events.
- The spatial prediction of landslide occurrence is still a major problem. Whereas large improvements have been made in modelling the flows related to landslide runout and debris flows, the accurate prediction of the landslide locations and landslide volumes still remains a challenge.
- The complexity of the hazard interactions might lead to unexpected results. For example a stronger rainfall event might lead to a lower hazard intensity than a relatively smaller event, because the peaks of the rainfall-runoff and sediment delivery might not coincide in the former, whereas they would in the latter event. This will also generate lower losses for the higher return period event, which is counterintuitive.
- Most of the integrated physically-based models are event-based, and require the rainfall and/or seismic acceleration of a single triggering event. The effect of antecedent precipitation and temperature conditions on the initial conditions at the start of the event-based simulation often have to be modeled separately.
- As the modelling time is often still considerable (depending on the size of the area, spatial and temporal resolution, and duration of the event), it is not feasible yet to use such models in a probabilistic manner, e.g. through the application of Monte Carlo simulation to account for the parameter uncertainty. Other approaches, such as ensemble modeling should be evaluated to

account for the uncertainty in the modelling. Also the link with probabilistic models for earthquakes or tropical storms, which analyze thousands of individual events, and evaluate the losses in a probabilistic manner, is still a challenge.

- The availability of vulnerability and fragility curves that can be linked to the outcome of the multi-hazard models is still rather limited. Progress has been made in generating databases of historical debris flow events for improving the generation of empirical curves for different building types and environments. Well documented vulnerability curves for a range of elements-at-risk in different environments should be collected on publicly available databases such as ERN-Vulnerability.
- Current risk assessment tools should developed more integrated links with the output of integrated physically-based multi-hazard landslide models. In generic risk assessment tools, such as RiskScape or RiskChanges, it might be easier to implements this. Probabilistic risk assessment tools, such as CAPRA, should consider how the results of these models can be integrated in a probabilistic approach.

The issues indicated above are not only relevant for analyzing the current level of risk, but also for analyzing changing risk, as a basis for decision making. Whereas multi-hazard risk assessments always are a multi-disciplinary exercises, requiring a wide range of expertise (from specific hazard modeling, to structural engineers, economist, social scientists, and geospatial experts), this range is further expands when analyzing risk dynamics. Climate experts, land use modelers, spatial planners, risk managers and other should work with the other experts in providing possible future scenarios, and risk reduction alternatives. This can only be carried out when the organizational structure is appropriate and when there is commitment from the various stakeholders. For example, in Medellin the National University of Colombia, the local government of Aburra Valley and initiatives as 100 Resilient cities (2020) have collaborated to characterize the potential hazards that can affect the different municipalities of the region and to strengthen the hydro meteorological and seismic monitoring of the catchments in the Aburra Valley through the project known as SIATA (100 Resilient cities, 2019). Medellin developed a strategy for resilience, in which two of the four main pillars are “sustainable and risk prepared Medellin” and “well-informed and engaged Medellin”. On the basis of this the city is strengthening community risk management,

retrofitting homes in informal settlements to improve living conditions, better incorporate them into the rest of the city and mitigate the city's exposure to the risk of landslides and earthquakes.

For the evaluation of “fast changes”, the ability to update existing information rapidly and continuously is one of the key requirements. In the case of impact-based forecasting, a series of loss scenarios could be worked out beforehand, that are correlated with a specific level of the trigger meteorological conditions. During the actual Early Warning phase the most likely scenario should then be determined on a continuous basis. Especially for multi-hazard risk assessment to support recovery planning it is essential to carry out rapid damage surveys using drones and collaborative mapping.

For the evaluation of “slow changes” related to scenarios of climate change, land use change and population change, stakeholder meetings are essential to determine the possible scenarios and future reference years. Also alternatives for multi-hazard mitigation should be defined for a specific area, which may incorporate a range of measures. Specific toolboxes for landslide mitigation measures, such as the one developed under the LaRIMIT project (LaRIMIT, 2020) might be very helpful. After these stakeholder meetings, there is a lot of homework for the individual experts. The consequences of the proposed scenarios are modeled in terms of changing return periods and land use, which forms the input for the hazard modelers, who's output again forms the input for risk modelers. Finally results of comparative risk assessment can be presented and discussed in stakeholder workshops, where decision are made or further modifications are proposed, leading again to a possible loop in the process. During such a process the availability of a Spatial Decision Support System that allows all stakeholders to provide their own piece, while still being able to oversee the whole jigsaw puzzle, is essential.

8 ACKNOWLEDGEMENTS

We would like to extend our thanks to the National University of Colombia and the Faculty of Mines-Medellin for their support in data collection and development of the example in Medellin, especially to Edier Aristizabal, Veronica Boter, Maria Isabel Arango, Sandra Lopez and the whole research group of Geohazards. We also thank the colleagues from the GeoInformatics Centre of the Asian Institute of Technology (AIT-GIC) with whom we developed the multi-hazard risk platform for Tajikistan: Kavinda Gunasekara, Manzul

Hazarika, Rajitha Athukorala, Tek Kshetri, Pratichya Sharma, Lakmal, Syams Nashrullah. Also the colleagues from Georgia (Tamo Tsamalashvili), Tajikistan (Sulaymon Shobek, Erkin Huseinov, Anatoly Ischuk, Nicolai Ischuk, Mirzo Saidov) and the Netherlands (Vasily Kokorev, and Janneke Ettema) are thanked for their input in developing the multi-hazard risk atlas for Tajikistan.

9 REFERENCES

- 100 Resilient Cities, 2019.
<http://100resilientcities.org/strategies/medellin/>
- Alcaldía de Envigado. (2018). Situación de salud 2017 del municipio de Envigado, 21–40
- Alford, D. (2000). Flood Scenarios. In D. Alford & R. L. Schuster (Eds.), *Usoi Landslide Dam and Lake Sarez: An assessment of hazard and risk in the Pamir Mountains, Tajikistan* (pp. 59–62). Geneva: United Nations Secretariat for International Strategy for Disaster Reduction.
- Alvioli, M., Melillo, M., Guzzetti, F., Rossi, M., Palazzi, E., von Hardenberg, J., Brunetti, M., Peruccacci, S. (2018) Implications of climate change on landslide hazard in Central Italy, *Science of The Total Environment*, Volume 630, 2018, Pages 1528-1543,
- AMVA (2006). Microzonificación Sísmica Detallada De Los Municipios De Barbosa, Girardota, Copacabana, Sabaneta, La Estrella, Caldas y Envigado, Informe Final. Área Metropolitana Del Valle de Aburrá, 745. <https://doi.org/10.4454/JPP.V96I2.031>
- AMVA. (2018). Estudios básicos de amenaza por movimientos en masa, inundaciones y avenidas torrenciales en los municipios de Caldas, la Estrella, Envigado, Itagüí, Bello, Copacabana y Barbosa, para la incorporación de la gestión del riesgo en la planificación territorial, 257.
- Anderson, L. Holcombe, R. Flory, J.-P. Renaud (2008) Implementing low-cost landslide risk reduction: a pilot study in unplanned housing areas of the Caribbean. *Natural Hazards*, 47 (3) (2008), pp. 297-315
- Aristizábal, E., Gonzalez, T., Montoya, J. D., Velez, J. I., Martinez, H., & Guerra, A. (2011). Analisis de umbrales empiricos de lluvia para el pronostico de moviemientos en masa en el Valle de Aburrá, Colombia. *Revista de La EIA*, 15(c), 95–111
- Aristizábal, E., Velez, J., & Martinez, H. (2016). Influences of antecedent rainfall and hydraulic conductivity on landslides triggered by rainfall occurrence using the model SHIA _ landslide, (65), 31–46
- Armenta, G., Dorado, J., Rodriguez, A., & Ruiz, J. (2014). Escenarios de Cambio Climático para precipitación y temperaturas en Colombia. Instituto de Hidrología, Meteorología y Estudios Ambientales de Colombia IDEAM

- Baum, R., Savage, W., & Godt, J. (2002). TRIGRS—a Fortran program for transient rainfall infiltration and grid-based regional slope-stability analysis. *US geological survey open-file report*, 424, 38.
- Bout, B., Lombardo, L., van Westen, C. J., & Jetten, V. G. (2018). Integration of two-phase solid fluid equations in a catchment model for flashfloods, debris flows and shallow slope failures. *Environmental Modelling & Software*, 105, 1-16.
- Bovolo, C.I., Abele, S.J., Bathurst, J.C., Caballero, D., Ciglan, M., Eftichidi, G., Simo, B., (2009). A distributed framework for multi-risk assessment of natural hazards used to model the effects of forest fire on hydrology and sediment yield. *Comput. Geosci.* 35, 924–945.
- Bruijn, K. de, Wagenaar, D., Slager, K., Bel, M. de, & Burzel, A. (2014). Updated and improved method for flood damage assessment, 2015(version 2)
- Byers, A. C., Rounce, D. R., Shugar, D. H., Lala, J. M., Byers, E. A., & Regmi, D. (2018). A rockfall-induced glacial lake outburst flood, Upper Barun Valley, Nepal. *Landslides*, 16(3), 533–549.
- Caballero, H. (1988). Algunos comentarios acerca del evento torrencial de la Quebrada Ayura (Envigado) y sus implicaciones en la amenaza del municipio. Ingeominas-Regional Medellin.
- CAPRA (2020) Probabilistic Risk Assessment Platform. <https://ecapra.org/>
- Clerici, A., & Perego, S. (2000). Simulation of the Parma River blockage by the Corniglio landslide (Northern Italy). *Geomorphology*, 33(1–2), 1–23.
- CHANGES. (2014). Changing Hydro-meteorological Risks – as Analyzed by a New Generation of European Scientists. Marie Curie Initial Training Network. <http://changes-itn.eu/>
- CHARIM, “Methods for Risk Assessment”, CHARIM Caribbean Handbook on Risk Information Management, University of Twente, 2016, <http://www.charim.net/methodology/55>.
- Chen, H. X., & Zhang, L. M. (2015). EDDA 1.0: integrated simulation of debris flow erosion, deposition and property changes. *Geoscientific Model Development*, 8(3), 829-844.
- Chen, H. X., Zhang, S., Peng, M., & Zhang, L. M. (2016). A physically-based multi-hazard risk assessment platform for regional rainfall-induced slope failures and debris flows. *Engineering geology*, 203, 15-29.
- Chen, L., van Westen, C. J., Hussin, H., Ciurean, R. L., Turkington, T., Chavarro-Rincon, D., & Shrestha, D. P. (2016). Integrating expert opinion with modelling for quantitative multi-hazard risk assessment in the Eastern Italian Alps. *Geomorphology*, 273, 150-167.
- Christen, M., Kowalski, J., & Bartelt, P. (2010). RAMMS: Numerical simulation of dense snow avalanches in three-dimensional terrain. *Cold Regions Science and Technology*, 63(1-2), 1-14.
- Ciurean, R. L., Hussin, H., Van Westen, C. J., Jaboyedoff, M., Nicolet, P., Chen, L., ... & Glade, T. (2017). Multi-scale debris flow vulnerability assessment and direct loss estimation of buildings in the Eastern Italian Alps. *Natural hazards*, 85(2), 929-957.
- Coe, J.A., Godt, J.W., 2012. Review of approaches for assessing the impact of climate change on landslide hazards. In: Eberhardt, E., et al. (Eds.), *Landslides and Engineered Slopes, Protecting Society Through Improved Understanding: Proceedings 11th International and 2nd North American Symposium on Landslides and Engineered Slopes*, Banff, Canada 1. Taylor & Francis Group, London, pp. 371–377
- Cohen, D., Lehmann, P., & Or, D. (2009). Fiber bundle model for multiscale modeling of hydromechanical triggering of shallow landslides. *Water resources research*, 45(10).
- Corominas, J., van Westen, C., Frattini, P., Cascini, L., Malet, J. P., Fotopoulou, S., ... Smith, J. T. (2014). Recommendations for the quantitative analysis of landslide risk. *Bulletin of Engineering Geology and the Environment*, 73(2), 209–263. <https://doi.org/10.1007/s10064-013-0538-8>
- COUPÉ, Françoise (2011). La gestión del riesgo en el Valle de Aburrá. una larga historia. *Gestión y Ambiente*, [S.I.], v. 14, n. 2, p. 17-44, mayo 2011. ISSN 2357-5905. Disponible en: <https://revistas.unal.edu.co/index.php/gestion/article/view/25469/39278>.
- DANE. (2019). Estimación y proyección de población nacional, departamental y municipal total por área 1985-2020. Retrieved August 27, 2018, from http://www.dane.gov.co/files/investigaciones/poblacion/proyepobla06_20/Municipal_area_1985-2020.xls
- De Graff, J.V. A rationale for effective post-fire debris flow mitigation within forested terrain. *Geoenvirom Disasters* 5, 7 (2018). <https://doi.org/10.1186/s40677-018-0099-z>
- Devoli, G., Tiranti, D., Cremonini, R., Sund, M., and Boje, S. (2018). Comparison of landslide forecasting services in Piedmont (Italy) and Norway, illustrated by events in late spring 2013, *Nat. Hazards Earth Syst. Sci.*, 18, 1351-1372
- Douglas, J., 2007. Physical vulnerability modelling for natural hazards risk assessment. *Nat. Hazards Earth Syst. Sci.* 7, 283–288.
- EM-DAT (2020): The Emergency Events Database - Université catholique de Louvain (UCL) - CRED, D. Guha-Sapir - www.emdat.be, Brussels, Belgium.
- Fan, X., Tang, C. X., Van Westen, C. J., & Alkema, D. (2012). Simulating dam-breach flood scenarios of the Tangjiashan landslide dam induced by the Wenchuan

- Earthquake. *Natural hazards and earth system sciences*, 12(10), 3031.
- Fan, L., Lehmann, P., McArdell, B., & Or, D. (2017). Linking rainfall-induced landslides with debris flows runoff patterns towards catchment scale hazard assessment. *Geomorphology*, 280, 1-15.
- Fan, X., Scaringi, G., Korup, O., West, A. J. , van Westen, C. J. , Tanyas, H., ... Huang, R. (2019). Earthquake-Induced Chains of Geologic Hazards: Patterns, Mechanisms, and Impacts. *Reviews of geophysics*, 1-83. <https://doi.org/10.1029/2018RG000626>
- Fan, X. , et al. (2020) The formation and impact of landslide dams – State of the art, *Earth-Science Reviews*,2020, 103116, ISSN 0012-8252,<https://doi.org/10.1016/j.earscirev.2020.103116>.
- FbF (2020) Forecast Based Financing. <https://www.forecast-based-financing.org/>
- Fell, R., Corominas, J., Bonnard, C., Cascini, L., Leroi, E., & Savage, W. Z. (2008). Guidelines for landslide susceptibility, hazard and risk zoning for land use planning. *Engineering Geology*, 102(3–4), 85–98. <https://doi.org/10.1016/j.enggeo.2008.03.022>
- FEMA (2020) HAZUS-MH analysis levels. Department of Homeland Security, Federal Emergency Management Agency. http://www.fema.gov/plan/prevent/hazus/hz_levels.shtm
- Florez, M. J., & Parra, L. (1988). Avalancha de la Querada Ayura del 14 de abril de 1988, 22
- Forzieri, G., Feyen, L., Russo, S., Vousdoukas, M., Alfieri, L., Outten, S., ... & Cid, A. (2016). Multi-hazard assessment in Europe under climate change. *Climatic Change*, 137(1-2), 105-119.
- Froude, M. and Petley, D. (2018). Global fatal landslide occurrence from 2004 to 2016. *Nat. Hazards Earth Syst. Sci.*, 18, 2161–2181, 2018 <https://doi.org/10.5194/nhess-18-2161-2018>
- Fuchs, S., Frazier, T. & Siebeneck, L. (2018) In *Vulnerability and Resilience to Natural Hazards* (eds Fuchs, S. & Taler, T.) 32–52 (Cambridge University Press, 2018)
- Gallina, V., Torresan, S., Critto, A., Sperotto, A., Glade, T., & Marcomini, A. (2016). A review of multi-risk methodologies for natural hazards: Consequences and challenges for a climate change impact assessment. *Journal of environmental management*, 168, 123-132.
- GAR (2015) Global Assessment Report on Disaster Risk Reduction, Data Platform. <https://risk.preventionweb.net/capreviewer/main.jsp?countrycode=g15>
- Garcia, C. (2006). Estado del conocimiento de los depositos de vertiente del Valle de Aburrá. *Boletin de Ciencias de La Tierra*, 19, 101–112
- Gariano, S.L., and F. Guzzetti, (2016): Landslides in a changing climate. *Earth-Science Rev.*, 162, 227–252
- GEM, (2020). OpenQuake Engine. User Instructions Manual. Global Earthquake Model. <https://docs.openquake.org/manuals/OpenQuake%20Manual%20%28latest%29.pdf>
- Gill, J. C., & Malamud, B. D. (2014). Reviewing and visualizing the interactions of natural hazards. *Reviews of Geophysics*, 52(4), 680-722.
- Gill, J. C., & Malamud, B. D. (2017). Anthropogenic processes, natural hazards, and interactions in a multi-hazard framework. *Earth-Science Reviews*, 166, 246-269.
- Godt, J., Sener, B., Verdin, K., Wald, D., Earle, P., Harp, E. and Jibson, R., (2008). Rapid assessment of earthquake-induced landsliding, *Proceedings of the First World Landslide Forum*, United Nations University, Tokyo, pp. 3166-1
- Glade T. (2003) Landslide occurrence as a response to land use change: a review of evidence from New Zealand. *Catena*. 2003;51:297–314
- Greiving, S., Fleischhauer, M., Wanczura, S. (2006): European Management of Natural Hazards: The Role of Spatial Planning in selected Member States. *Journal of Environmental Planning and Management*. Vol. 49, No. 5, September 2006, S. 739 – 757.
- Hermelin, M.; Toro, G. y Velásquez, A., (1984). Génesis de los depósitos de vertiente en el sur del Valle de Aburrá. *Resúmenes I Conferencia sobre Riesgos Geológicos en el Valle de Aburrá*
- Hor bath, J. E. (2016). Tendencias y proyecciones de la población del área metropolitana del Valle de Aburrá en Colombia, 2010-2030. *Notas de Población* (Vol. 43). <https://doi.org/10.18356/9d3ffa22-es>
- Horton, P., Jaboyedoff, M., Rudaz, B. E. A., & Zimmermann, M. (2013). Flow-R, a model for susceptibility mapping of debris flows and other gravitational hazards at a regional scale. *Natural hazards and earth system sciences*, 13(4), 869-885.
- Hsu, W. K., Huang, P. C., Chang, C. C., Chen, C. W., Hung, D. M., & Chiang, W. L. (2011). An integrated flood risk assessment model for property insurance industry in Taiwan. *Natural Hazards*, 58(3), 1295-1309.
- Huggel, C., J.J. Clague, and O. Korup, 2012: Is climate change responsible for changing landslide activity in high mountains? *Earth Surf. Process. Landforms*, 37, 77–91
- Hurtado, A.I. and Yamin, L. (2018) CAPRA Landslide Toolbox. <https://ecapra.org/topics/landslide-toolbox>

- IPCC. (2012). Managing the risks of extreme events and disasters.
<https://doi.org/10.1017/CBO9781139177245>
- IPCC, (2019): Climate Change and Land.
<https://www.ipcc.ch/srcc/>
- Jong, S. M. De, & Jetten, V. G. (2007). Estimating spatial patterns of rainfall interception from remotely sensed vegetation indices and spectral mixture analysis Article, (May 2014).
<https://doi.org/10.1080/13658810601064884>
- Kappes, M. S., Keiler, M., von Elverfeldt, K., & Glade, T. (2012). Challenges of analyzing multi-hazard risk: a review. *Natural hazards*, 64(2), 1925-1958.
- Kirschbaum, D. and Stanley, T. (2018), Satellite-Based Assessment of Rainfall-Triggered Landslide Hazard for Situational Awareness. *Earth's Future*. .
 doi:10.1002/2017EF000715
- Koliji, A. (2008). Geotechdata.info. Retrieved January 28, 2019, from [http://www.geotechdata.info/About us.html](http://www.geotechdata.info/About%20us.html)
- Komatitsch, D., Göddeke, D., Erlebacher, G., & Michéa, D. (2010). Modeling the propagation of elastic waves using spectral elements on a cluster of 192 GPUs. *Computer Science-Research and Development*, 25(1-2), 75-82.
- Komendatova, N., Mrzyglocki, R., Mignan, A., Khazai, B., Wenzel, F., Patt, A., & Fleming, K. (2014). Multi-hazard and multi-risk decision-support tools as a part of participatory risk governance: Feedback from civil protection stakeholders. *International Journal of disaster risk reduction*, 8, 50-67.
- Kuriakose, S. L., Devkota, S., Rossiter, D. G., & Jetten, V. G. (2009). Prediction of soil depth using environmental variables in an anthropogenic landscape, a case study in the Western Ghats of Kerala, India. *Catena*, 79(1), 27-38.
- LaRIMIT (2020). LaRiMit (Landslide Risk Mitigation Toolbox) is an Expert-Based Landslide Mitigation Portal to identify cost-effective structural and non-structural landslide risk mitigation option.
<https://www.larimit.com/>
- Lee, K. T., & Ho, J. Y. (2009). Prediction of landslide occurrence based on slope-instability analysis and hydrological model simulation. *Journal of Hydrology*, 375(3-4), 489-497.
- Liu, Z., Nadim, F., Garcia-Aristizabal, A., Mignan, A., Fleming, K., & Luna, B. Q. (2015). A three-level framework for multi-risk assessment. *Georisk: Assessment and Management of Risk for Engineered Systems and Geohazards*, 9(2), 59-74.
- Malek, Ž., Douw, B., Van Vliet, J., Van Der Zanden, E. H., & Verburg, P. H. (2019). Local land-use decision-making in a global context. *Environmental Research Letters*, 14(8), 1-14.
- Marzocchi, W., Mastellone, M., Di Ruocco, A., Novelli, P., Romeo, E., & Gasparini, P. (2009). Principles of multi-risk assessment: interactions amongst natural and man-induced risks. *European Commission, Directorate-General for Research, Environment Directorate*.
- Marzocchi, W., Sandri, L., & Selva, J. (2010). BET_VH: a probabilistic tool for long-term volcanic hazard assessment. *Bulletin of volcanology*, 72(6), 705-716
- Marzocchi, W., Garcia-Aristizabal, A., Gasparini, P., Mastellone, M.L., Di Ruocco, A., 2012. Basic principles of multi-risk assessment: a case study in Italy. *Nat. Hazards* 62, 551–573
- Mergili, M., Schneider, D., Worni, R., & Schneider, J. F. (2011). Glacial Lake Outburst Floods in the Pamir of Tajikistan: Challenges in Prediction and Modelling. *Italian Journal of Engineering Geology and Environment - Book*, 973–982.
<https://doi.org/10.4408/IJEGE.2011-03.B-106>
- Mergili, M., Marchesini, I., Rossi, M., Guzzetti, F., & Fellin, W. (2014). Spatially distributed three-dimensional slope stability modeling in a raster GIS. *Geomorphology*, 206, 178-195.
- Mergili, M., Fischer, J. T., & Pudasaini, S. P. (2017). Process chain modelling with r. avaflow: lessons learned for multi-hazard analysis. In *Workshop on World Landslide Forum*(pp. 565-572). Springer, Cham.
- Mergili, M., Jan-Thomas, F., Krenn, J., & Pudasaini, S. P. (2017). r. avaflow v1, an advanced open-source computational framework for the propagation and interaction of two-phase mass flows. *Geoscientific Model Development*, 10(2), 553.
- Mergili, M., Emmer, A., Juřicová, A., Cochachin, A., Fischer, J. T., Huggel, C., & Pudasaini, S. P. (2018). How well can we simulate complex hydro-geomorphic process chains? The 2012 multi-lake outburst flood in the Santa Cruz Valley (Cordillera Blanca, Perú). *Earth Surface Processes and Landforms*.
- Ministerio de Ambiente Vivienda y Desarrollo Territorial. (2004). Decreto 2060 de 2004, (2060), 1–2
- MunichRe. (2020) <https://www.munichre.com/topics-online/en/2018/01/2017-year-in-figures> and <https://www.munichre.com/topics-online/en/climate-change-and-natural-disasters/natural-disasters/the-natural-disasters-of-2018-in-figures.html>
- Narasimhan, H., Ferlisi, S., Cascini, L., De Chiara, G., & Faber, M. H. (2016). A cost-benefit analysis of mitigation options for optimal management of risks posed by flow-like phenomena. *Natural Hazards*, 81, 117–144. <https://doi.org/10.1007/s11069-015-1755-1>
- Newman, J. P., Maier, H. R., Riddell, G. A., Zecchin, A. C., Daniell, J. E., Schaefer, A. M., ... & Newland, C. P. (2017). Review of literature on decision support systems for natural hazard risk reduction: Current

- status and future research directions. *Environmental Modelling & Software*, 96, 378-409.
- Nowicki Jessee, M.A., Hamburger, H.W., Allstadt, K.E., Wald, D.J., Robeson, S.M., Tanyas, H., Hearne, M., Thompson, E.M., (2018), A Global Empirical Model for Near Real-time Assessment of Seismically Induced Landslides, *J. Geophys. Res.*
- O'Brien, J. S., Julien, P. Y., & Fullerton, W. T. (1993). Two-dimensional water flood and mudflow simulation. *Journal of hydraulic engineering*, 119(2), 244-261.
- Papathoma-Köhle, M. (2016). Vulnerability curves vs. vulnerability indicators: application of an indicator-based methodology for debris-flow hazards. *Nat. Hazards Earth Syst. Sci.*, 16, 1771–1790,
- Papathoma-Köhle, M. Gems,B. Sturm,M., Fuchs, S. (2017) Matrices, curves and indicators: A review of approaches to assess physical vulnerability to debris flows, *Earth-Science Reviews*, Volume 171, 2017, 272-288,
- Peduto, D., Ferlisi, S., Nicodemo, G. et al. (2017) Empirical fragility and vulnerability curves for buildings exposed to slow-moving landslides at medium and large scales. *Landslides* 14, 1993–2007
- Piciullo, L., Calvello, M., and Cepeda, J. M. (2018). Territorial early warning systems for rainfall-induced landslides, *Earth-Sci. Rev.*, 179, 228–247
- POT (2011). Plan de Ordenamiento Territorial Envigado 2011-2023. Retrieved from <http://www.suenosytierras.com/biblioteca/Envigado-P.O.T-ACUERDO-010-2011.pdf>
- Pirotti, F et al. (2015). <http://doi.org/10.1007/978-3-662-45931-7>
- Promper,C., A. Puissant, J.-P. Malet, T. Glade,(2014) Analysis of land cover changes in the past and the future as contribution to landslide risk scenarios, *Applied Geography*, Volume 53, 2014, 11-19,
- Reese, S.; Bell, R.G. and King, A.B. (2007). RiskScape - A new tool for comparing risk from natural hazards. *Water & Atmosphere*, 15 (3): 24-25.
- Reid, M. E., Christian, S. B., Brien, D. L., & Henderson, S. T. (2015). Scoops3D—Software to Analyze Three-dimensional Slope Stability Throughout a Digital Landscape. In *Tech. Rep. US Geological Survey Techniques and Methods, book 14* (p. 218).
- Schmidt, J., Matcham, I., Reese, S., King, A., Bell, R., Henderson, R., ... & Heron, D. (2011). Quantitative multi-risk analysis for natural hazards: a framework for multi-risk modelling. *Natural Hazards*, 58(3), 1169-1192.
- Schneider, P. J., & Schauer, B. A. (2006). HAZUS—its development and its future. *Natural Hazards Review*, 7(2), 40-44.
- Tanyas, H., Rossi, M., Alvioli, M. , van Westen, C. J., & Marchesini, I. (2019). A global slope unit-based method for the near real-time prediction of earthquake-induced landslides. *Geomorphology*, 327, 126-146.
- Terzi, S., Torresan, S., Schneiderbauer, S., Critto, A., Zebisch, M., & Marcomini, A. (2019). Multi-risk assessment in mountain regions: A review of modelling approaches for climate change adaptation. *Journal of environmental management*, 232, 759-771.
- UNDRR (2020). Sendai Framework for Disaster Risk Reduction. <https://www.undrr.org/implementing-sendai-framework/what-sf>
- USGS (2020). Ground Failure Model background <https://earthquake.usgs.gov/data/ground-failure/background.php#refs>
- Uzielli, M., Nadim, F., Lacasse, S., & Kaynia, A. M. (2008). A conceptual framework for quantitative estimation of physical vulnerability to landslides. *Engineering Geology*, 102(3-4), 251-256.
- Van Beek LPH, Van Asch TWJ. (2004) Regional assessment of the effects of land-use change on landslide hazard by means of physically based modelling. *Nat Hazards*.;31:289–304
- van Westen, C. J., van Asch, T. W. J., & Soeters, R. (2006). Landslide hazard and risk zonation : why is it still so difficult? *Bulletin of engineering geology and the environment*, 65(2), 167-184.
- van Westen, C. (2014). Analyzing Changing Risk and Planning Alternatives : a Case Study of a Small Island Country . Enschede, Netherlands: University of Twente- Faculty of Geo-Information and Earth Observation (ITC). <https://doi.org/10.13140/RG.2.2.18620.03204>
- van Westen, C. J., & Greiving, S. (2017). Multi-hazard risk assessment and decision making. *Environmental Hazards Methodologies for Risk Assessment and Management*, 31.
- Van Westen et al., (2020). Multi-hazard risk profiles at district level for Tajikistan. <http://tajirisk.ait.ac.th/>
- Von Ruette, J., Lehmann, P., & Or, D. (2013). Rainfall-triggered shallow landslides at catchment scale: Threshold mechanics-based modeling for abruptness and localization. *Water Resources Research*, 49(10), 6266-6285.
- .Zhang, K. et al. (2016) iCRESTRIGRS: a coupled modeling system for cascading flood–landslide disaster forecasting. *Hydrol. Earth Syst. Sci.*, 20, 5035–5048, 2016
- Zobel, C.W. and Khansa, L. (2014) Characterizing multi-event disaster resilience. <https://doi.org/10.1016/j.cor.2011.09.024>